

IDENTIFICATION OF GALACTIC BULGE SURVEY X-RAY SOURCES WITH TYCHO-2 STARS

ROBERT I. HYNES^{1,2}, N. J. WRIGHT³, T. J. MACCARONE⁴, P. G. JONKER^{5,6,3}, S. GREISS⁷, D. STEEGHS^{7,3}, M. A. P. TORRES^{5,3}, C. T. BRITT², G. NELEMANS⁶

Submitted to the Astrophysical Journal Supplement

ABSTRACT

We identify 69 X-ray sources discovered by the Galactic Bulge Survey (GBS) that are coincident with, or very close to bright stars in the Tycho-2 catalog. Additionally, two other GBS sources are resolved binary companions to Tycho-2 stars where both components are separately detected in X-rays. Most of these are likely to be real matches, but we identify nine objects with large and significant X-ray to optical offsets as either detections of resolved binary companions or chance alignments. We collate known spectral types for these objects, and also examine 2MASS colors, variability information from the All-Sky Automated Survey (ASAS), and X-ray hardness ratios for the brightest objects. Nearly a third of the stars are found to be optically variable, divided roughly evenly between irregular variations and periodic modulations. All fall among the softest objects identified by the GBS. The sample forms a very mixed selection, ranging in spectral class from O9 to M3. In some cases the X-ray emission appears consistent with normal coronal emission from late-type stars, or wind emission from early-types, but the sample also includes one known Algol, one W UMa system, two Be stars, and several X-ray bright objects likely to be coronally active stars or binaries. Surprisingly, a substantial fraction of the spectroscopically classified, non-coincidental sample (12 out of 38 objects) have late B or A type counterparts. Many of these exhibit redder near-IR colors than expected for their spectral type and/or variability, and it is likely that the X-rays originate from a late-type companion star in most or all of these objects.

Subject headings: surveys — stars: activity — stars: massive — stars: emission-line, Be — binaries: close

1. INTRODUCTION

The Galactic Bulge Survey (GBS; Jonker et al. 2011) is a wide but shallow X-ray survey of two strips above and below the bulge. The design of the survey calls for two regions of Galactic longitude $-3^\circ < l < 3^\circ$, and latitude $1^\circ < |b| < 2^\circ$. Three quarters of the area was imaged by the *Chandra X-ray Observatory* ACIS-I camera with exposures of at least 2 ks and a detection flux limit of $7.7 \times 10^{-14} \text{ erg cm}^{-2} \text{ s}^{-1}$ from 2007–2009, with the remaining area being observed in Fall 2011 and Spring 2012. This has resulted in the detection of 1234 X-ray sources from the 2007–2009 observations (Jonker et al. 2011) and an additional 424 objects from 2011–2012 (Jonker et al., in preparation). By design, the survey avoids the most crowded and absorbed regions of the Galactic plane and so many of these sources have unique candidate optical counterparts. Follow-up optical spectroscopy and multi-epoch photometry is finding a high fraction of sources with spectroscopic peculiar-

ities and/or photometric variability that appear to be true counterparts to the X-ray sources. Most sources are expected to be Galactic in origin, although about some background active galactic nuclei are present in the sample (Maccarone et al. 2012).

Among the optical counterparts, a fraction correspond to very bright, often nearby stars, and these can be expected to be dominated by detections of ‘normal’ stars. This paper reports on the properties of those GBS objects coincident with stars in the Tycho-2 catalog (Høg et al. 2000a). As such, it is limited to optical counterparts brighter than 12th magnitude. Many of these stars also appear in the Henry Draper catalogs (Cannon & Pickering 1918–1924; Cannon 1925–1936; Nesterov et al. 1995) and so have spectral classifications. While our main interest is to find any abnormal objects among the sample, by matching of our predominantly faint X-ray sources with bright optical counterparts we are naturally selecting for objects with rather low X-ray to optical flux ratios, and will thus expect to mainly exclude exotica like X-ray binaries.

While there were isolated early detections of stellar X-rays, the *Einstein* satellite really opened the door to systematic studies of stellar X-ray emission, and revealed that across the Hertzsprung-Russell diagram X-ray sources are the rule, rather than the exception (Vaiana et al. 1981). As the sensitivity of X-ray telescopes has improved, more and more stars have been added to X-ray catalogs, consequently filling in the region of parameter space occupied by the lowest X-ray luminosity stars. In some cases this is through deliberate surveys, and sometimes as serendipitous detections. A comprehensive review of stellar X-ray astronomy is pro-

¹ E-mail: rih@phys.lsu.edu

² Department of Physics and Astronomy, Louisiana State University, 202 Nicholson Hall, Tower Drive, Baton Rouge, LA 70803, USA

³ Harvard-Smithsonian Center for Astrophysics, 60 Garden Street, Cambridge, MA 02138, U.S.A.

⁴ School of Physics and Astronomy, University of Southampton, Southampton SO17 1BJ, United Kingdom

⁵ SRON, Netherlands Institute for Space Research, Sorbonnelaan 2, 3584 CA, Utrecht, The Netherlands

⁶ Department of Astrophysics, IMAPP, Radboud University Nijmegen, Heyendaalseweg 135, 6525 AJ, Nijmegen, The Netherlands

⁷ Astronomy and Astrophysics, Department of Physics, University of Warwick, Coventry, CV4 7AL, United Kingdom

vided by Güdel & Nazé (2009) and references therein.

Among early-type OB stars, the standard paradigm is that X-rays arise from shocks within their strong winds at quite large radii (Owocki & Cohen 2001, and references therein). Empirically, the relation $L_X/L_{\text{bol}} \simeq 10^{-7}$ is found in O–B1 stars (Pallavicini et al. 1981; Berghöfer et al. 1997), supporting a strong coupling between the radiatively driven winds and the X-ray generation. Many details of the mechanism remain unclear, and the high spectral resolution studies possible with *Chandra* and *XMM-Newton* have raised challenges to the standard paradigm (e.g. Pollock 2007). The X-ray spectra from these objects are typically very soft, peaking below 1.5 keV. They can usually be well fit by between one and three thermal plasma components (e.g. Sana et al. 2006; Antokhin et al. 2008). In reasonably close OB binaries, it is possible to also develop X-rays from the shock where their winds interact, leading to the class of over-luminous colliding wind binaries (Stevens et al. 1992).

The efficiency of X-ray production from winds drops substantially among B stars, with L_X/L_{bol} decreasing from 10^{-6} for the most X-ray luminous B0 stars to 10^{-10} – 10^{-8} for spectral types later than B2 (Cohen et al. 1997). Sana et al. (2006) found that in the young open cluster NGC 6231 less than 20% of mid to late B stars were detected in X-rays, and those that were had harder spectra than the O stars, and were sometimes seen to flare. They suggested that the X-rays actually originate from pre-main-sequence companions, for which the hard spectra and flaring are quite typical.

The Be stars form an important sub-class of B stars (Porter & Rivinius 2003). In these rapidly rotating stars an equatorial excretion disk develops. These objects can be intrinsic X-ray emitters in their own right, with typical Be stars in the sample of Cohen et al. (1997) showing X-ray luminosities about three times higher than comparable normal B stars. More dramatically, when Be star systems play host to neutron stars, more luminous X-rays from the interaction between the compact object and the circumstellar material can be seen, typically in periodic outbursts (Coe 2000). Recently a class of intermediate luminosity objects, the γ Cas analogs, have been identified (Motch et al. 2007) including, it turns out, one of our sample, HD 161103 (Lopes de Oliveira et al. 2006). These objects show much harder X-ray spectra than typical OB or Be stars, and short timescale X-ray variability. Their nature remains unclear; they could be unusual single Be stars, or counterparts to the Be X-ray binaries containing white dwarfs instead of neutron stars.

X-ray emission from solar- and late-type main sequence stars is ubiquitous and originates from a magnetically confined plasma at a temperature of several million Kelvin known as a corona (Vaiana et al. 1981). The corona is powered by a dynamo, which itself is generated by a combination of rotation and convection within the convective envelope. A strong correlation between rotation and stellar X-ray activity was first noted by Pallavicini et al. (1981) and has since been quantified in detail (e.g. Wright et al. 2011), providing strong support for the dynamo-induced nature of stellar activity. As stars spin down as they age (e.g. Skumanich 1972), the dynamo weakens and X-ray activity reduces from the high levels seen in young stars ($L_X/L_{\text{bol}} \sim 10^{-3}$, e.g.

Feigelson et al. 2005) to the levels typically seen in the Sun and old field stars ($L_X/L_{\text{bol}} \sim 10^{-5} - 10^{-7}$, e.g. Wright et al. 2010). Generally late-type evolved stars are weak X-ray emitters. Exceptions can be expected to be unusually rapidly rotating single stars, of which the FK Com stars present the most extreme example, or forced into rapid rotation in close binaries such as RS CVn systems. A comprehensive review of X-ray emission from stellar coronae is provided by Güdel (2004).

In fully radiative stars (earlier than mid F-type) the dynamo mechanism breaks down and X-ray emission becomes very weak. Vega, for example, remains undetected as an X-ray source, with a *Chandra* upper limit to its luminosity of 2×10^{25} erg s $^{-1}$ (Pease et al. 2006). X-ray detections of late B and A stars are then quite unexpected, and in most cases the origin of the X-rays will be a later type companion star.

More generally, the overarching scientific interest of the GBS is to extend our knowledge of binaries, and binary evolution, and as discussed above, we would expect many of the X-ray brightest objects in our sample to be binaries in some form. RS CVn systems have already been mentioned. BY Dra systems are similar, containing main-sequence stars. Algols, too are typically seen as X-ray emitters, with the X-rays originating from the cooler star in the binary. The most extreme close binaries, contact W UMa systems, are also expected to have strong coronal X-ray emission. The Algols illustrate an important point. Here, it is commonly the hotter component that is seen in the optical spectrum, but the cool component that gives rise to coronal X-rays. Generally, we cannot always assume that the optically brightest star is the X-ray source.

The goals of this paper are to summarize the matches between the GBS and Tycho-2 stars, to discuss their properties and attempt to classify each object, to examine if any of these stars show anomalous X-ray emission for their spectral type, and ultimately to either identify objects containing compact companions or eliminate these objects from our sample as candidate interacting binaries. We begin by discussing the catalogs and matching criteria used in Section 2. To classify the sources we then examine X-ray to optical flux ratios (Section 3), optical/infrared color-color diagrams (Section 4), and X-ray hardness ratios (Section 5). We draw this, and other available information together for individual sources in Section 6, and finally discuss the classes of objects found in Section 7 and summarize our findings in Section 8.

2. OPTICAL AND INFRARED COUNTERPARTS TO GBS X-RAY SOURCES

2.1. Duplicate X-ray detections

Our starting point is the X-ray source lists from the GBS. We merge the published list, which we will refer to as the northern sample (Jonker et al. 2011) with additional sources detected in the final southern strip of the survey, the southern sample (Jonker et al. in preparation). For ease of recognition we will use abbreviated source names of CXnnnn for sources from the northern sample, and CXBnnnn for sources in the southern sample. Besides being more compact, this notation has the advantage that each list is sorted in order of X-ray brightness, so the CX number conveys information that is absent from the longer positional names such as CX-

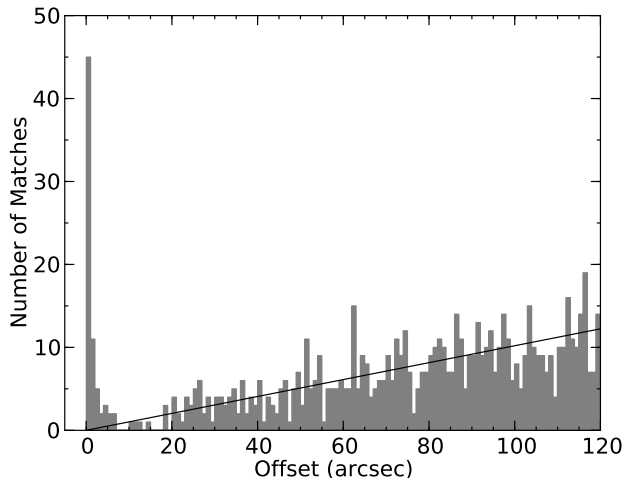


Figure 1. Number of matches found between GBS X-ray sources and stars in the Tycho-2 catalog, as a function of offset. Bins are 1 arcsec wide. The solid line is the expected number of chance coincidences based on the number of matches found with offsets of 1–15 arcmin.

OGBS J175024.4–290216.

In performing our optical matches, we identified two cases where two of the X-ray sources appear to coincide with the same Tycho star. In both cases, the two X-ray sources were detected in different images, and one has a much larger off-axis angle than the other, and consequently less precise coordinates. In these cases we believe that they are duplicate detections of the same source, with position differences just too large for Jonker et al. (2011) to have identified them as duplicates. The redundant sources are CX191, which appears to have been an off-axis detection of CX360, and CX230, which appears to be an off-axis detection of CX33. Another similar case has been found with the optically fainter cataclysmic variable candidate CX93, for which CX153 appears to be an off-axis detection (Ratti et al. in preparation). On examination of the GBS source catalog, we identified a further fifteen likely duplications which share the characteristics of being from different Chandra observation IDs and having one or both detection at sizeable off-axis angle. These are: CX16 = CX515, CX38 = CX225, CX61 = CX136, CX175 = CX464, CX177 = CX384, CX345 = CX233, CX270 = CX571, CX597 = CX273, CX280 = CX382, CX394 = CX285, CX292 = CX323, CX304 = CX303, CX1155 = CX483, CX636 = CX635, and CX646 = CX851. In each case, we have listed the detection with smallest off-axis angle first, so the second source of each pair can be considered the duplicate. In most cases, the detection closer to the axis is also the stronger one. A few more cases were found where close objects appear to be detected in the same observation ID, and we believe these are distinct X-ray sources. CX916 and CX917 are one such pair that match an optical double, HD316666A and B. We removed all eighteen of the apparent duplicate objects from the catalog leaving 1216 unique sources in the northern sample.

Following this experience, we were careful to check the southern sample for repeat detections of objects from the northern sample, and for duplicates. As a result, the southern sample includes 424 new and unique X-ray

sources with no credible duplications. After duplicate removal, our combined catalogs total 1640 unique sources. All statistics reported here on numbers of matches expected and found are based on this combined unique subset of the full source lists.

2.2. Matches with the Tycho-2 and Henry Draper Catalogs

We primarily consider matches with the Tycho-2 Astrometric Catalog (Høg et al. 2000a). This provides a reasonably uniform catalog of the 2.5 million brightest stars in the sky, with excellent positions and lower quality, although still useful, two color photometry. We also check for matches with the original Henry Draper Catalog (Cannon & Pickering 1918–1924), the Henry Draper Catalog Extension (Cannon 1925–1936), and the Henry Draper Extension Charts (see Nesterov et al. 1995, and references therein) as these provide spectroscopic classifications for many of the matches found in the Tycho-2 Catalog.

We consider a candidate match to be an X-ray source within 10 arcsec of a Tycho-2 star to allow for the large uncertainties in *Chandra* positions for large off-axis angles (see Hong et al. 2005). Proper motions are applied to the Tycho-2 stars pair-by-pair to obtain the correct optical coordinates corresponding to the epoch of each Chandra observation. The proper motions between the J2000 reference epoch of the Tycho-2 catalog, and the 2006–2012 Chandra observations are mostly small compared to the Chandra positional uncertainty, but not always, with the largest accumulated proper motion (for CXB93, a nearby M dwarf) being 3.3 arcsec.

We identify 70 Chandra sources that lie within 10 arcsec of 69 Tycho-2 stars (both CX916 and CX917 lie close to the same star; see below). Information about these matches is summarized in Table 1 for the objects from Jonker et al. (2011) and Table 2 for the southern objects from Jonker et al. (in preparation). Most of these actually match to within 1 arcsec, with a few at substantially larger deviations: the median X-ray/optical offset is 0.60 arcsec, while the mean offset is 1.19 arcsec. After removing the ten objects identified as either chance coincidences or alignments with resolved companions (see Section 2.3), the median X-ray/optical offset drops to 0.49 arcsec, and the mean to 0.74 arcsec. These numbers are consistent with the absolute astrometric calibration of *Chandra*, for which the 90% uncertainty is 0.6 arcsec⁸.

Of these sources, 28 also clearly coincide with a source in one of the Henry Draper catalogs. In addition in one case, CX77, the positional offset between the Tycho-2 position and the nearest HD star, HD159571 is 45 arcsec, but the photometry of the two stars agree. The discrepancy cannot be due to proper motion as the Tycho-2 star only has a proper motion of 2.9 mas yr⁻¹. Examining Digital Sky Survey images of the region, there is no bright star at the quoted position of HD159571, so we believe the coordinates quoted are inaccurate and count this as a match, in agreement with Fabricius et al. (2002).

Finally, we identify two additional GBS sources with resolved companions to X-ray detected Tycho-2 stars. CX917 appears to coincide with HD316666B, the com-

⁸ <http://cxc.harvard.edu/cal/ASPECT/celmon/>

Table 1
Bright Optical Counterparts to GBS Northern Sources

| GBS | Tycho-2 | HD | Offset (arcsec) | V | $(B - V)$ | $\log(F_x/F_{\text{opt}})$ | Spectral Type | Refs. |
|------|--------------|---------|--------------------|------------------|--------------------|----------------------------|---------------|----------|
| 4 | 6839-00084-1 | 316072 | 0.46 | 9.93 ± 0.03 | 1.21 ± 0.07 | -2.54 | G9 III | 1 |
| 6 | 6836-00576-1 | 161103 | 0.21 | 8.40 ± 0.01 | 0.33 ± 0.02 | -3.34 | B0.5 III-ve | 2, 3 |
| 7 | 6839-00513-1 | ... | 0.30 | 11.20 ± 0.10 | 0.88 ± 0.19 | -2.23 | K0 V | 1 |
| 9 | 6839-00257-1 | 315997 | 0.30 | 11.36 ± 0.11 | 0.32 ± 0.14 | -2.20 | A5 | 4 |
| 10 | 6839-00191-1 | 315992 | 0.46 | 10.13 ± 0.04 | 1.10 ± 0.08 | -2.75 | G7 | 4, 5 |
| 12 | 7377-01129-1 | 318207 | 0.11 | 9.46 ± 0.02 | 1.09 ± 0.04 | -3.10 | G5 | 4 |
| 25 | 7381-00792-1 | ... | 0.56 | 11.76 ± 0.17 | 0.85 ± 0.29 | -2.50 | ... | ... |
| 26 | 7377-00936-1 | 161212 | 0.14 | 8.87 ± 0.02 | 0.64 ± 0.03 | -3.65 | G3 V | 6 |
| 27 | 6839-00636-1 | ... | 0.80 | 12.19 ± 0.23 | 0.63 ± 0.36 | -2.33 | ... | ... |
| 31 | 6839-00348-1 | ... | 0.10 | 9.97 ± 0.03 | 0.47 ± 0.05 | -3.25 | O9 V | 7 |
| 32 | 6839-00218-1 | ... | 0.34 | 10.97 ± 0.08 | 0.66 ± 0.11 | -2.83 | ... | ... |
| 33 | 6840-01414-1 | 316341 | 0.08 | 9.10 ± 0.02 | 0.50 ± 0.03 | -3.62 | B0 ve | 8 |
| 53 | 6836-01113-1 | 161117 | 3.33 | 8.85 ± 0.02 | 0.39 ± 0.02 | -3.88 | F5 V | 6 |
| 59 | 6832-00663-1 | ... | 3.53 | 10.24 ± 0.05 | 0.35 ± 0.06 | -3.35 | ... | ... |
| 72 | 7377-00222-1 | 316356 | 0.18 | 10.40 ± 0.06 | 0.37 ± 0.08 | -3.36 | F8 | 4 |
| 77 | 6839-00487-1 | 159571 | 6.32 | 9.05 ± 0.02 | 0.11 ± 0.02 | -3.90 | B8 V | 6 |
| 82 | 6849-01294-1 | ... | 0.97 | 12.32 ± 0.19 | 0.49 ± 0.28 | -2.58 | ... | ... |
| 91 | 6849-01082-1 | 314883 | 1.11 | 10.58 ± 0.05 | 0.47 ± 0.06 | -3.35 | F8 | 4 |
| 115 | 6839-00265-1 | 316070 | 0.60 | 9.98 ± 0.03 | 0.36 ± 0.04 | -3.66 | A2 | 4 |
| 156 | 6840-01006-1 | 161907 | 6.24 | 8.05 ± 0.01 | 0.28 ± 0.02 | -4.48 | F0 V | 6 |
| 183 | 6840-01069-1 | 162120 | 1.04 | 8.34 ± 0.01 | 0.18 ± 0.02 | -4.43 | A2V | 6 |
| 205 | 7377-00199-1 | 161852 | 1.63 | 6.65 ± 0.01 | 0.32 ± 0.02 | -5.18 | F2 IV/V | 6 |
| 256 | 6853-00214-1 | 162761 | 0.26 | 7.89 ± 0.01 | 1.08 ± 0.02 | -4.77 | K0 III | 6 |
| 272 | 6836-00635-1 | ... | 0.82 | 11.53 ± 0.14 | 0.81 ± 0.26 | -3.32 | ... | ... |
| 275 | 6835-00321-1 | 160627 | 1.96 | 8.11 ± 0.01 | 0.36 ± 0.02 | -4.69 | F0 V | 6 |
| 296 | 6840-01244-1 | 316432 | 0.38 | 11.99 ± 0.26 | 0.11 ± 0.30 | -3.18 | F0 | 4 |
| 333 | 6839-00340-1 | 159509 | 1.55 | 9.69 ± 0.03 | 0.42 ± 0.04 | -4.10 | A4 III | 6 |
| 337 | 6839-00205-1 | 315995 | 1.08 | 10.88 ± 0.08 | 0.24 ± 0.09 | -3.63 | A0 | 4 |
| 352 | 6853-00288-1 | 316675 | 0.34 | 12.03 ± 0.33 | -0.22 ± 0.33^a | -3.23 | F8 | 4 |
| 360 | 6840-00525-1 | ... | 4.07 | 11.11 ± 0.12 | 0.65 ± 0.18 | -3.60 | ... | ... |
| 388 | 6839-00615-1 | ... | 4.79 | 11.51 ± 0.15 | 0.39 ± 0.19 | -3.44 | ... | ... |
| 402 | 7376-00402-1 | 316033 | 0.68 | 9.99 ± 0.04 | 0.91 ± 0.06 | -4.04 | G5 | 4 |
| 452 | 7377-00626-1 | ... | 0.24 | 11.04 ± 0.12 | 1.63 ± 0.40 | -3.69 | ... | ... |
| 467 | 6835-00391-1 | ... | 0.84 | 10.07 ± 0.04 | 0.58 ± 0.07 | -4.08 | ... | ... |
| 485 | 6839-00212-1 | 316059 | 0.03 | 10.48 ± 0.05 | 0.60 ± 0.07 | -3.92 | F8 | 4 |
| 506 | 6835-00186-1 | 160390 | 0.33 | 9.32 ± 0.02 | 0.41 ± 0.03 | -4.34 | A2/A3 III | 6 |
| 514 | 6849-01034-1 | 314884 | 1.47 | 10.04 ± 0.03 | 0.01 ± 0.03 | -4.17 | B9 | 4 |
| 524 | 6853-00080-1 | ... | 0.78 | 10.46 ± 0.08 | 1.30 ± 0.21 | -4.00 | ... | ... |
| 622 | 6839-00019-1 | ... | 2.37 | 11.66 ± 0.18 | 0.73 ± 0.30 | -3.52 | ... | ... |
| 632 | 6838-01055-1 | 315998 | 1.28 | 9.81 ± 0.03 | 1.43 ± 0.08 | -4.26 | K1 III | 5 |
| 680 | 6853-01070-1 | ... | 0.44 | 11.35 ± 0.18 | 0.54 ± 0.26 | -3.74 | ... | ... |
| 698 | 6853-01354-1 | ... | 0.49 | 11.52 ± 0.18 | 0.25 ± 0.21 | -3.67 | ... | ... |
| 728 | 7377-00394-1 | ... | 2.68 | 11.29 ± 0.14 | 1.34 ± 0.39 | -3.76 | ... | ... |
| 768 | 7377-00310-1 | ... | 0.47 | 11.41 ± 0.15 | 1.91 ± 0.50 | -3.72 | ... | ... |
| 785 | 6835-00311-1 | 160769 | 0.54 | 8.86 ± 0.02 | 0.42 ± 0.03 | -4.74 | F3 V | 6 |
| 863 | 6838-00781-1 | 158902 | 0.39 | 7.23 ± 0.01 | 0.29 ± 0.02 | -5.39 | B3-5 Ia/b-II | 6, 9, 10 |
| 904 | 6849-01144-1 | ... | 0.67 | 11.25 ± 0.09 | 0.73 ± 0.14 | -3.91 | ... | ... |
| 916 | 6849-00227-1 | 316666A | 0.73 | 10.06 ± 0.05 | 0.34 ± 0.06 | -4.38 | F0 | 4 |
| 925 | 6849-00157-1 | ... | 2.84 | 10.68 ± 0.09 | 1.04 ± 0.19 | -4.13 | ... | ... |
| 1087 | 6835-00082-1 | ... | 0.80 | 10.89 ± 0.09 | 0.71 ± 0.13 | -4.05 | ... | ... |
| 1092 | 6835-00596-1 | ... | 0.20 | 10.88 ± 0.09 | 0.79 ± 0.14 | -4.06 | ... | ... |
| 1113 | 6835-00312-1 | ... | 0.53 | 11.73 ± 0.16 | 0.53 ± 0.22 | -3.68 | ... | ... |
| 1219 | 7376-00879-1 | ... | 0.14 | 11.18 ± 0.13 | 0.92 ± 0.24 | -3.94 | ... | ... |

References. — (1) Torres et al. (2006) (2) Steele et al. (1999), (3) Lopes de Oliveira et al. (2006), (4) Nesterov et al. (1995), (5) Siebert et al. (2011), (6) Houk (1982), (7) Vijapurkar & Drilling (1993), (8) Levenhagen & Leister (2006), (9) MacConnell & Bidelman (1976), (10) Garrison et al. (1977),

^a This color is almost certainly spurious due to strong variability in this object.

panion to HD 316666A (CX916). CXB36 coincides with HD 318327B, the companion to HD 318327A (CXB93).

2.3. Chance coincidences

With the precise localization possible with *Chandra*, we expect few of our matches to be coincidences with bright stars. We can assess the probability of chance coincidences by comparing the number of matches between GBS X-ray sources and Tycho-2 stars within a specified matching radius to the number of matches found within an annulus around the X-ray source. This preserves in-

formation about the spatial distributions of X-ray and optical sources to provide a robust estimate, for this region of the sky, of the probability of a chance coincidence.

We plot the number of matches found as a function of offset in Figure 1. The central peak contains 45 candidate matches with offsets below 1 arcsec, 11 with offsets of 1–2 arcsec, and 14 with offsets of 2–7 arcsec. There are no candidate matches between 7–10 arcsec, so we have a total of 70 candidate matches with Tycho-2 stars. Comparing this central peak in the distribution with the number found at larger radii it is clear that few can be ex-

Table 2
Bright Optical Counterparts to GBS Southern Strip Sources

| GBS | Tycho-2 | HD | Offset (arcsec) | V | $(B - V)$ | $\log(F_x/F_{\text{opt}})$ | Spectral Type | Refs. |
|------|--------------|---------|--------------------|------------------|------------------|----------------------------|---------------|-------|
| B5 | 7375-00399-1 | 315961 | 0.14 | 10.17 ± 0.05 | 1.12 ± 0.10 | -2.95 | K5 | 1 |
| B9 | 7377-01107-1 | 161853 | 0.67 | 7.95 ± 0.01 | 0.13 ± 0.02 | -3.85 | O8 III | 2 |
| B17 | 6853-01752-1 | 316565 | 4.98 | 10.62 ± 0.09 | 0.53 ± 0.12 | -3.10 | F8 | 1 |
| B93 | 7381-00585-1 | 318327A | 0.49 | 10.66 ± 0.07 | 1.04 ± 0.13 | -3.62 | M3 v | 3 |
| B116 | 6849-01175-1 | 314886 | 0.27 | 10.19 ± 0.03 | 0.36 ± 0.04 | -3.92 | A5 | 1 |
| B128 | 6832-00621-1 | ... | 1.42 | 9.89 ± 0.04 | 0.51 ± 0.05 | -4.06 | ... | ... |
| B181 | 6853-00523-1 | 162962 | 0.35 | 9.95 ± 0.05 | 0.84 ± 0.08 | -4.16 | A0 | 4 |
| B200 | 7376-00433-1 | ... | 0.42 | 12.07 ± 0.22 | 0.24 ± 0.29 | -3.31 | ... | ... |
| B211 | 7381-00288-1 | 160826 | 2.61 | 8.51 ± 0.01 | 0.07 ± 0.02 | -4.73 | B9 v | 5 |
| B225 | 6853-03032-1 | ... | 2.51 | 11.01 ± 0.09 | 0.44 ± 0.12 | -3.83 | ... | ... |
| B233 | 6853-00479-1 | 316692 | 1.13 | 10.21 ± 0.06 | -0.01 ± 0.06 | -4.15 | A0 | 1 |
| B287 | 7376-00194-1 | 158982 | 1.39 | 9.40 ± 0.02 | 0.27 ± 0.03 | -4.48 | A2 IV/V | 5 |
| B296 | 7377-00827-1 | 161839 | 5.95 | 9.63 ± 0.03 | 0.11 ± 0.04 | -4.51 | B5/7 II/III | 5 |
| B302 | 6849-01627-1 | ... | 0.42 | 11.87 ± 0.17 | 0.39 ± 0.22 | -3.61 | ... | ... |
| B306 | 6853-00059-1 | 163613 | 0.39 | 8.56 ± 0.01 | 0.25 ± 0.02 | -4.94 | B1 I-II | 6 |
| B422 | 7375-00782-1 | 315956 | 0.60 | 9.66 ± 0.03 | 0.43 ± 0.04 | -4.52 | F2 | 1 |

References. — (1) Nesterov et al. (1995), (2) Parthasarathy et al. (2000) (3) Raharto et al. (1984), (4) Cannon & Mayall (1949), (5) Houk (1982), (6) Hoffleit (1956),

pected to be coincidences. Statistically we would expect ~ 5 chance coincidences within 10 arcsec, a 20% chance of finding one match within 2 arcsec, and a 5% chance of finding one within 1 arcsec. Given these statistics it seems likely that a few of the matches with offsets of 2–7 arcsec are due to chance coincidence, but most are probably not. In some cases the match may be with a resolved binary companion rather than to the Tycho-2 star itself.

Those sources observed by Chandra at small off-axis angles with good detections are most suspect. We can assess the likelihood of a chance match on a case-by-case basis using the results of Hong et al. (2005) who present 95% confidence radii as a function of off-axis angle and number of counts. Of the offsets greater than 2 arcsec, CX917 can immediately be excluded as this corresponds to the resolved companion HD316666B, and the large offset comes from matching it with HD316666A. We find that the offsets for CX728, CX925, CXB211, and CXB225 are not significant at the 95% confidence level so these may be true counterparts to the X-ray source observed at large off-axis angles. For the remainder of the objects with offsets greater than 2 arcsec, in every case the offset is at least twice the 95% confidence ranges so these nine objects (CX53, 59, 77, 156, 360, 388, 622, and CXB17, and 296) are either matches with resolved binary companions or true coincidences.

We also checked the ten objects with offsets between 1 and 2 arcsec by the same criteria. All of these objects were observed at greater than 5 arcmin off-axis angle, and none of the offsets seen are significant at the 95% confidence level, so we believe these are all true matches, as was expected statistically.

2.4. Spectral types

The first step in obtaining a credible classification for the objects found is a spectral type for the optical counterpart. The Henry Draper Catalog, Extension, and Charts provide a baseline classification but this is often crude and lacks luminosity classes. For objects in the original Henry Draper Catalog, improved classifications with luminosity classes are available in the Michigan Cat-

alogue of two-dimensional spectral types for the HD stars (Houk 1982). We also checked each object against the on-line Catalog of Stellar Classifications (Skiff 2011) and for a number of objects, especially the handful of early-type stars, one or more modern classifications were available. Where we list no spectral types in Table 1 or 2, we could find no published spectral classification in the literature.

2.5. Infrared counterparts from 2MASS

We also collate infrared photometry of our objects from the Two Micron All Sky Survey (Skrutskie et al. 2006, 2MASS). While in general the GBS is working with the superior IR data from the Vista Variables in the Via Lactea project (Saito et al. 2012, VVV), for the objects considered here, VVV photometry is expected to be saturated and so 2MASS is generally more reliable.

2.6. Variability from ASAS

Finally we checked each matched Tycho-2 star against the All Sky Automated Survey (ASAS) Catalog of variable stars (Pojmanski 2002). Our findings are summarized in Table 3. We found seven matches with identified ASAS variables: CX4, CX6, CX9, CX33, CX352, CXB287, and CXB422. Of these, CX6 and CX352 are known variables (V3892 Sgr and V779 Sgr respectively), and CX33 was a previously suspected variable (NSV 23882). CX9 is attributed a 5.72 day period in the ASAS catalog, but we could not reproduce this. Otero et al. (2006) instead find a period of 2.87 days (almost, but not quite, half the ASAS period) which we can reproduce. We were not able to confirm the putative variability in either CXB287, or CXB422 using the ASAS data.

To place limits on the variability present in each of the other objects, we also examined the ASAS photometry of each one. We show in Fig. 2 a measure of the scatter of the lightcurves as a function of magnitude. All of our Tycho-2 stars were included in the ASAS photometry database, although the brightest are saturated and unusable. CX205 is by far the worst case at magnitude 6.7. CX156, CX183, CX256, CX275, and CX863

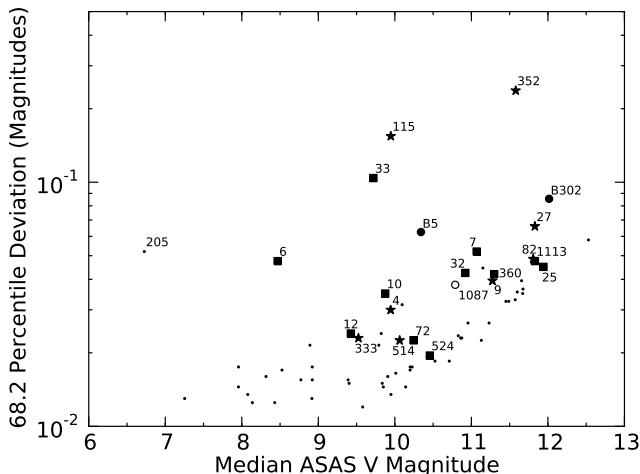


Figure 2. Strength of variability in ASAS lightcurves as a function of magnitude. 68.2% of points lie within 1 deviation of the median. Solid stars are objects showing periodic variability, solid squares show apparently real aperiodic variability, and open circles show excess variance for their magnitude, but not compelling pattern of variability in their lightcurve. Note that CX205 is not variable but is beyond the saturation limit of the ASAS survey.

all suffer from mild saturation but we can still exclude large amplitude variability in these objects. We initially used the standard deviation of the lightcurves to quantify the variability (considering only A grade photometry), but found that there were several objects showing large standard deviations caused by a small number of points with large excursions several magnitudes below the typical values. Many stars show these excursions, even well understood objects such as the W UMa system V3892 Sgr (CX352), so we believe they are spurious. We opt to instead quantify the variance by measuring the deviation from the median enclosing 68.2% of the points. For a Gaussian distribution this is equal to the standard deviation, but it is more robust to the presence of small numbers of outliers with extremely large deviations. Using this statistic, the plot became much cleaner than using the standard deviation.

Several variables showed up in this way that were not included in the ASAS variability catalog, most notably V846 Oph (CX115), a known eclipsing Algol. We also performed a visual examination of all lightcurves as a function of time, and a period search. For each object, we filter the data by the grade of photometry, typically keeping just grades A and B. Period searches were carried out separately for 1–100 days, and 2–24 hours using Lomb-Scargle periodograms, and verified by inspection of both unbinned and binned folded lightcurves. In this process, we picked up another four periodic variables that had not passed the ASAS acceptance criteria: CX27, CX82, CX333, and CX514, are all low-amplitude, periodic systems. CX7, CX10, CX12, CX25, CX32, CX72, CX360, CX524, CX1113, and CXB5 all show irregular variability of some form, either slow trends, irregular flickering-like behavior, or in the case of CX72 a single discrete outburst. Our final test was to examine Lomb-Scargle periodograms of each year of data separately. This is useful where a period may not be coherent on long timescales, for example if the starspot geometry on a star is changing. Only one periodic variable was added to the list,

CX7, which showed quite complex behavior. We will discuss this in Section 6.4.

There remain several objects for which the variance is larger than typical for stars of their magnitude, but for which we could not confirm real variability in the lightcurve. The most pronounced cases are CX1087, CXB17, CXB200, and CXB296. These objects may show unresolved short timescale variability. We note that both CXB17 and CXB296 appear to be chance coincidences with Tycho-2 stars.

In all, we identify 9 periodic variables, 5 definite irregular ones, and a further 7 suspected irregular variables. Two X-ray bright objects, CX4 and CX7, show both periodic and aperiodic behavior. In total, a third (20/60) of the non-coincidental matches appear to be variable in ASAS data. This is probably an underestimate given the presence of other objects which appear to show an excess variance compared to other stars at a similar magnitude, but neither a detectable period, nor clear, resolved aperiodic variability.

3. FLUX RATIOS

Ratios of X-ray to optical flux provide a very useful diagnostic of whether X-ray emission can be attributed to normal stellar activity (in winds from early type stars and coronae of late type stars), or require a more exotic explanation. Such diagnostics are very crude in the absence of spectral information as there are then uncertainties in the nature of the optical star, its bolometric flux, and the amount of optical extinction and X-ray absorption. Nonetheless, as a crude cut we show the optical to X-ray flux ratio as a function of $B-V$ and $J-K$ colors in Fig. 3.

A group of stars stands out in both diagrams as having high F_X/F_{opt} relative to the remainder. These are CX4, 7, 9, 10, 12, 25, 27, 82, and CXB5. In defining these, we have simply picked the outliers in Figure 3, and have not tried to set an arbitrary cut-off in $\log(F_{\text{opt}}/F_V)$.

CX9 is an A star in an eclipsing binary. As we will discuss, we suspect this is an Algol system. CX7 is a K0 star that was identified as a pre-main-sequence star by Torres et al. (2006). CX4 appears to be a rapidly rotating G9 giant. The X-rays are likely coronal with strong activity driven by rapid rotation. All three of these objects for which we have classifications appear to be unusual objects in some respect. CX25, CX27, and CX82 have similar F_X/F_{opt} ratios, so these too are probably unusual objects warranting further attention. CX10, CX12, and CXB5 are also outliers. As will discuss in Section 5, this group of sources besides being among the brighter objects in our sample, also have the hardest spectra, excluding the massive stars, and as we have seen several of these are also variable.

A few stars appear to have anomalous colors. CX352 is continuously variable, so all of its colors are suspect unless taken at the same orbital phase, or phase-averaged. CX452, 728, 768, and 1219 all have redder optical colors than expected based on their IR color (see Section 4) and so their Tycho-2 $B-V$ colors are suspect. They are not strong outliers when plotted in $J-K$. CXB296 is a strong outlier when plotted against $J-K$ only due to its very strong IR excess. This is suspected to be a Be star, but in any case appears to be a chance alignment with CXB296.

Table 3
ASAS Counterparts to Optically Bright GBS Sources

| GBS | ASAS | 68.2% Variance | Period (Days) | Comments |
|------|---------------|-------------------|------------------|-------------------------------------|
| 4 | 173931-2909.9 | 0.030 | 16.0834(55) | Previously identified ASAS variable |
| 6 | 174446-2713.7 | 0.047 | ... | Known Be variable, V3892 Sgr |
| 7 | 173826-2901.8 | 0.052 | ... | New ASAS variable |
| 9 | 173508-2923.5 | 0.039 | 2.87233(14) | Previously identified ASAS variable |
| 10 | 173629-2910.5 | 0.035 | ... | New ASAS variable |
| 12 | 174347-3140.4 | 0.024 | ... | New ASAS variable |
| 25 | 174503-3159.6 | 0.045 | ... | New ASAS variable |
| 26 | 174533-3058.9 | 0.016 | ... | |
| 27 | 173653-2848.7 | 0.066 | 31.132(30) | New ASAS variable |
| 31 | 173804-2907.1 | 0.013 | ... | |
| 32 | 174105-2815.1 | 0.043 | ... | New ASAS variable |
| 33 | 174836-2957.5 | 0.104 | ... | Previously identified ASAS variable |
| 53 | 174449-2635.3 | 0.015 | ... | |
| 59 | 174500-2612.5 | 0.017 | ... | |
| 72 | 174820-3028.6 | 0.022 | ... | New ASAS variable |
| 77 | 173638-2859.9 | 0.018 | ... | |
| 82 | 175710-2725.4 | 0.048 | 6.299(33) | New ASAS variable |
| 91 | 175611-2714.5 | 0.016 | ... | |
| 115 | 173941-2851.2 | 0.154 | 3.12678(14) | Known eclipsing Algol, V846 Oph |
| 156 | 174928-2918.9 | 0.013 | ... | |
| 183 | 175041-2916.7 | 0.016 | ... | |
| 205 | 174917-3035.8 | 0.052 | ... | |
| 256 | 175348-2841.3 | 0.018 | ... | |
| 272 | 174354-2701.7 | 0.035 | ... | |
| 275 | 174205-2650.7 | 0.013 | ... | |
| 296 | 174951-2956.2 | 0.035 | ... | |
| 333 | 173618-2834.3 | 0.023 | 14.6565(48) | New ASAS variable |
| 337 | 173527-2930.8 | 0.023 | ... | |
| 352 | 175537-2818.1 | 0.237 | 0.44503030(36) | Known W UMa variable, V779 Sgr |
| 360 | 175114-2919.2 | 0.042 | ... | New ASAS variable |
| 388 | 173700-2906.1 | 0.023 | ... | |
| 402 | 173533-3023.6 | 0.013 | ... | |
| 452 | 174546-3108.5 | 0.032 | ... | |
| 467 | 174124-2657.9 | 0.014 | ... | |
| 485 | 173719-2829.4 | 0.018 | ... | |
| 506 | 174046-2801.8 | 0.016 | ... | |
| 514 | 175637-2711.8 | 0.022 | 0.889524(27) | New ASAS variable |
| 524 | 175419-2836.9 | 0.019 | ... | New ASAS variable |
| 622 | 173654-2952.7 | 0.037 | ... | |
| 632 | 173354-2923.9 | 0.015 | ... | |
| 680 | 175412-2839.3 | 0.032 | ... | |
| 698 | 175221-2904.5 | 0.039 | ... | |
| 728 | 174812-3024.5 | 0.058 | ... | |
| 768 | 174438-3114.2 | 0.033 | ... | |
| 785 | 174250-2750.6 | 0.022 | ... | |
| 863 | 173303-2939.1 | 0.013 | ... | |
| 904 | 175624-2710.4 | 0.026 | ... | |
| 916 | 175542-2804.4 | 0.021 | ... | |
| 925 | 175450-2753.6 | 0.019 | ... | |
| 1087 | 174141-2736.8 | 0.038 | ... | |
| 1092 | 174110-2647.1 | 0.023 | ... | |
| 1113 | 174012-2802.2 | 0.048 | ... | New ASAS variable |
| 1219 | 173317-3020.7 | 0.022 | ... | |
| B5 | 173209-3028.5 | 0.062 | ... | New ASAS variable |
| B9 | 174917-3115.3 | 0.015 | ... | |
| B17 | 175430-2923.9 | 0.032 | ... | |
| B93 | 174613-3206.1 | 0.018 | ... | |
| B116 | 175708-2708.9 | 0.024 | ... | |
| B128 | 174651-2546.8 | 0.014 | ... | |
| B181 | 175455-2912.2 | 0.016 | ... | |
| B200 | 173351-3050.5 | 0.045 | ... | |
| B211 | 174329-3213.9 | 0.013 | ... | |
| B225 | 175619-2828.2 | 0.026 | ... | |
| B233 | 175521-2834.4 | 0.018 | ... | |
| B287 | 173334-3032.0 | 0.015 | ... | |
| B296 | 174909-3117.3 | 0.024 | ... | |
| B302 | 175841-2754.1 | 0.086 | ... | New ASAS variable |
| B306 | 175810-2808.5 | 0.017 | ... | |
| B422 | 173117-3019.3 | 0.012 | ... | |

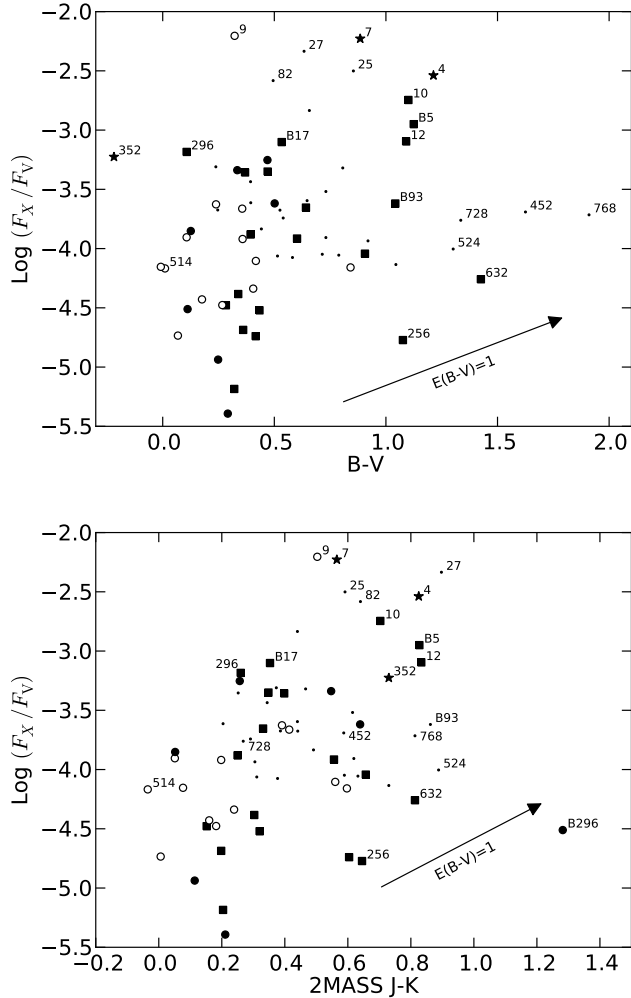


Figure 3. Relation between X-ray to optical flux ratio and optical color (upper) and IR color (lower). Stars with no spectral classification are shown with points. Of the remainder, filled circles indicate O and early B stars, open circles late B and A stars, stars are unusual late type stars, and squares are late type stars with no variability or other noted peculiarities. We label selected objects only for clarity. These are mainly outliers from the distribution. The arrows indicate the effect of a reddening of $E(B - V) = 1$ on the color and flux ratio for an assumed 10 MK APEC spectrum.

The bottom left of this diagram is populated by massive OB stars and A stars. Most of the objects falling in this region already have spectral classifications, and it is likely that we have identified all of the OB stars in the sample. This is not surprising, as OB stars are a rare population for which considerable effort has been expended in optical observations to identify members. Some of the unclassified stars may be A stars, but it is likely that the majority are mid- to late-type stars, with unremarkable F_X/F_{opt} ratios suggesting normal coronal emission.

For the stars for which we have spectral types, and even better, luminosity classes, these diagnostics become more powerful. Knowing the spectral type of the star, we can deduce its bolometric flux using standard relations from Cox (2000). We can also compare observed and intrinsic colors to deduce the reddening, $E(B - V)$, and hence estimate the interstellar X-ray absorption using the scaling of Bohlin et al. (1978): $N_{\text{H}} = 5.8 \times 10^{21} \text{ cm}^{-2} \times E(B - V)$.

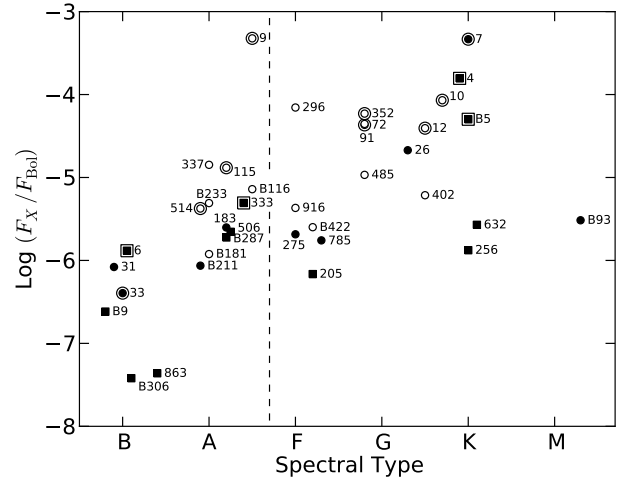


Figure 4. Relation between X-ray to bolometric flux ratio as a function of spectral type for those stars with full (spectral and luminosity) or partial (spectral only) classifications. Filled squares are evolved stars, filled circles are main-sequence stars, and open circles are stars with no luminosity classification. Objects with an outer circle or square are identified variables. Objects with high X-ray/optical offsets that are most likely to be chance alignments have been omitted. The vertical dashed line is drawn for a spectral type of A7, to indicate the cut-off of expected coronal X-ray emission from the visible star.

We convert *Chandra* count rates to absorption-corrected fluxes using PIMMS. We assume a 10 MK APEC spectrum⁹ and evaluate the unabsorbed flux as a function of absorption column. 10 MK was chosen not only as representative of stellar coronal temperatures, but as roughly the temperature at which ACIS-I is most sensitive to coronal spectra. As a result, the flux calculated assuming a 10 MK spectrum should provide a robust lower limit to the flux (and hence the flux ratio) expected for hotter or cooler coronae.

Using this information we then plot in Fig. 4 the absorption-corrected ratio of X-ray to bolometric luminosity as a function of spectral-type. We indicate on this figure a vertical line at spectral type A7, marking the effective cut-off of coronal activity. It is notable that there is a cluster of sources with late-B and A spectral types in the gap that should exist between the OB and Be stars to the left, and the coronal stars to the right. Of these, CX9 stands out by more than an order of magnitude compared to the others. We also note the very pronounced tendency for the stars with high F_X/F_{Bol} ratios to be variable, with CX296 as a notable exception. Since the optical counterpart to CX296 is among the faintest in our sample, it is quite possible its variability is undetectable in the ASAS data.

4. COLOR-COLOR DIAGRAMS

We combine Tycho-2 and 2MASS colors in Fig. 5 to examine possible deviations from the colors of a single star. Tycho-2 photometry has been converted into the *UBV* system using the transformations of Høg et al. (2000b), while 2MASS photometry is left in its own *JHK_S* system. We also overlay main-sequence colors taken from

⁹ <http://www.atomdb.org>

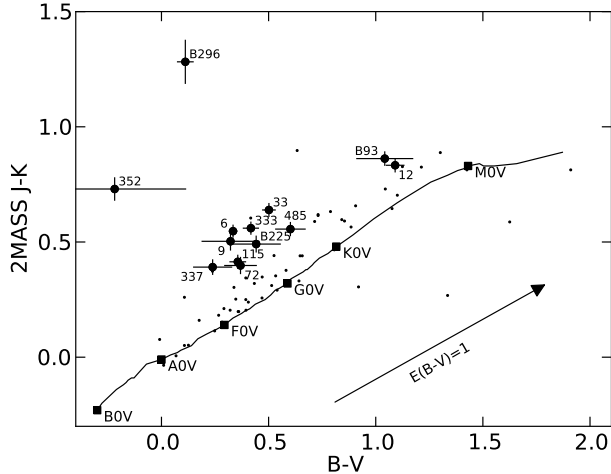


Figure 5. Optical/IR color-color diagram. Tycho-2 photometry has been converted to the standard UBV system, 2MASS photometry is left in its own system. We overlay main-sequence colors for comparison. All points are shown, but for clarity we only show error bars and labels on those points lying more than 3σ from the line. The arrow shows the effect of reddening by $E(B - V) = 1$ for the extinction curve of Cardelli et al. (1989).

the online compilation of Eric Mamajek¹⁰.

The sources generally scatter around the stellar lines, although with many more objects above the lines than below them, corresponding to IR colors that are redder than expected based on optical colors. This cannot be explained by interstellar reddening as dereddening the colors will take them further from the stellar lines. It most probably indicates a cooler IR excess, either from a cooler companion star (in most cases) or from a circumstellar disk in the case of Be stars. In a few cases the colors may be compromised by variability. CX352 is the worst case as it has a continuously variable large-amplitude lightcurve, and its Tycho-2 colors are bluer than expected from its spectral type. The other large amplitude variable is the eclipsing Algol CX115. In this case, it is possible colors are valid if they were obtained out of eclipse, and we certainly expect a cool companion to be present since it is an Algol system.

Unfortunately for many of our objects the Tycho-2 colors are too uncertain to draw strong conclusions about individual objects (although the statement that more sources lie above the line than below it stands in a statistical sense). We select those individual objects which lie more than 3σ from either line for further consideration, and highlight them in Fig. 5. All of the objects below the line fail this test, since they all have large color uncertainties. The remaining outliers are all above the line, corresponding to unusually red infrared colors. The outliers are CX6, CX9, CX12, CX33, CX72, CX115, CX333, CX337, CX352, CX485, CXB93, CXB225, and CXB296.

We immediately discount CX352 as compromised by variability. CX6 and CX33 are both known Be stars so are expected to have an infrared excess from a circumstellar disk. HD 161839 appears to only be a coincidental match with CXB296, but also has a very large infrared excess (seen beyond the 2MASS bands). CX115 is an Al-

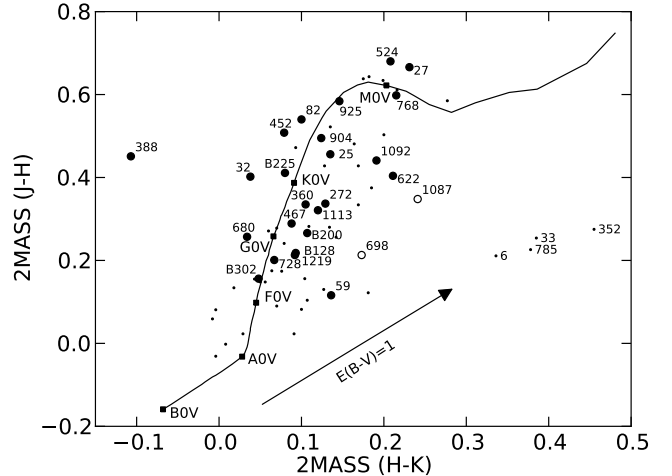


Figure 6. Infrared color-color diagram. We overlay main-sequence colors for comparison. All points are shown, but for clarity we only show labels on objects that do not have a spectral classification, or that are strong outliers. Open circles are objects for which the 2MASS photometry is flagged as suspect. The arrow shows the effect of reddening by $E(B - V) = 1$ for the extinction curve of Cardelli et al. (1989). Main sequence colors are indicated following the compilation of Eric Mamajek (see text).

gol system, so should have a cooler companion star. Of the others, CX9, CX333, and CX337 are in the A star clump in Fig. 4. All are objects for which negligible intrinsic X-ray emission is expected, and so the presence of a cooler companion is naturally to be expected. CX12, CX72, and CX485 are late F to G stars with rather high F_X/F_{Bol} ratios and so it is also quite credible that these are active binaries with cooler companions.

An additional diagnostic that is independent of uncertainties in the Tycho-2 photometry is a $J - H$ versus $H - K$ IR color-color diagram (Figure 6). This exploits changes in the shape of the JHK portion of the spectrum as a function of spectral class (Straizys & Lazauskaitė 2009). This also is more sensitive to the nature of a cool component. We show the main-sequence line of Eric Mamajek (see above), and note that giants tend to be redder in $J - H$ than main-sequence stars, so will fall higher in the diagram (Straizys & Lazauskaitė 2009). Most objects lie on the stellar line or to the right of it (due to reddening) as expected. The group of outliers to the far right is a mixed group. CX6 and CX33 are both Be stars with dust emission. CX352 is a large amplitude variable. The other outliers to the right have suspect 2MASS photometry. There is no obvious explanation for the location of CX388 to the left of the diagram, although we note this star is likely a chance coincidence in any case. Among the objects with no spectral classification and good 2MASS photometry, all plausible matches with GBS objects show IR colors consistent with lightly reddened FGKM stars, suggesting that in all or most of these cases the X-rays originate from a coronally active late type star. This supports our earlier suggestion that we have likely identified all of the OB stars in this sample.

5. HARDNESS RATIOS

For the majority of our sources we do not have useful X-ray spectra. *Chandra* is not optimized for spectroscopy with the short exposures we are using, so those

¹⁰ http://www.pas.rochester.edu/~emamajek/EEM_dwarf_UBVIJHK_colors_Teff.dat

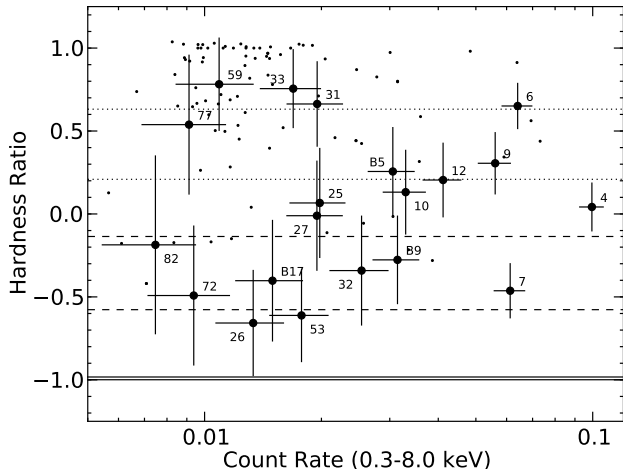


Figure 7. Hardness ratios of the brightest sources. Our hardness ratios are defined as the 1.25–8.0 keV rate minus 0.3–1.25 keV rate divided by the 0.3–8.0 keV rate. Note that this is a softer definition than Jonker et al. (2011) use. We show only those sources for which more than 20 counts were recorded. Sources considered in this work have uncertainties plotted and are annotated. Other sources are shown by points only to reduce the clutter of the plot. The solid lines are 1 MK APEC spectra, the dashed lines are 10 MK APEC spectra, and the dotted lines are 40 MK APEC spectra. For each pair, the lower line has zero absorption, the upper line has to $N_{\text{H}} = 5.8 \times 10^{21} \text{ cm}^{-2}$ corresponding to $E(B - V) = 1$.

sources with large enough count rates to yield a useful spectrum in just 2 ks tend to be quite piled up, compromising the spectral information. We can, however, extract useful hardness ratios for the brightest sources in the GBS, and this was done by Jonker et al. (2011) for the northern sample. The objects considered here with Tycho-2 counterparts were among the softest detected, with all having negative hardness ratios as defined by Jonker et al. (2011), so for this work we recalculated hardness ratios for both samples to provide better discrimination amongst soft sources. The definition we use is the difference between the 1.25–8.0 keV count rate and the 0.3–1.25 keV rate divided by the whole 0.3–8.0 keV rate. We calculate these ratios for all sources for which more than 20 photons are detected, and show these data in Fig. 7 with the Tycho-2 sources highlighted. We also show hardness ratios for a number of combinations of coronal temperature and absorption for comparison.

We can see immediately that, as noted above, the Tycho-2 sources are amongst the softest in the GBS. This is as expected if they are dominated by stellar coronal emission. Conversely, most of the bright, soft sources detected by the GBS have Tycho-2 counterparts. The hardest sources in our sample include CX6 and CX33, both of which are Be stars; CX31 which is also a massive star; and CX59 and CX77 both of which were flagged as possible chance alignments with a larger than expected difference between X-ray and optical positions.

The next group in hardness are CX4, CX9, CX10, CX12, CX25, CX27, and CXB5. Strikingly all of these objects were highlighted in Section 3 as objects with the highest $F_{\text{X}}/F_{\text{opt}}$ ratios. All have late spectral types, or colors consistent with late types (except CX9 for which a late-type companion is indicated by eclipses), and so these appear to be active objects with luminous, hot

coronae.

6. INDIVIDUAL OBJECTS

6.1. Source Distances and Locations

In a few cases *Hipparcos* parallaxes exist for our optical counterparts. These provide good estimates of distance, and hence X-ray luminosity (Table 4). In the absence of a parallax distance, if we have a spectral and luminosity classification then we can estimate a spectroscopic parallax distance (Table 5). To do this we use intrinsic $(B - V)$ colors from Fitzgerald (1970) to estimate $E(B - V)$, and then absolute magnitudes from Straižys & Kuriliene (1981) to derive a distance. In the absence of a luminosity class, we can obtain a lower limit on the distance by assuming a main-sequence star.

For the non-*Hipparcos* objects for which we estimate $E(B - V)$ based on spectral classifications, we also list the Bulge reddening estimated by Gonzalez et al. (2011) and Gonzalez et al. (2012) based on red clump stars in VVV data. In every case, our inferred reddening is much less than the Bulge reddening, consistent with the relatively short distances deduced for these objects. Note that this is also true for the early-type stars at inferred distances of several kiloparsecs.

Where appropriate, we will discuss the location of the more distant (non-local) sources. We assume the distance of the Sun from the Galactic center is $8.33 \pm 0.35 \text{ kpc}$ (Gillessen et al. 2009). We adopt a distance of the Sun above the plane of $26 \pm 3 \text{ pc}$ (Majaess et al. 2009). These numbers are of some importance as we are conducting a Bulge survey, not a plane survey, and so our lines of sight diverge from the plane at larger distances. Consequently, we would only expect to see relatively nearby early-type stars in our sample, at least among the higher latitude sources (e.g. CX863, CXB9, CXB306). The spiral structure of the Milky Way along our sightlines can be seen in the maps of Churchwell et al. (2009). Beyond the local stars of the Orion Spur, we encounter the Sagittarius Arm at around 1.2 kpc, the Scutum-Centaurus Arm around 2.8 kpc, the Norma Arm around 4.4 kpc, and the Near 3 kpc Arm around 5.8 kpc. Among the luminous stars considered here, the Be stars CX6 and CX33 (and the coincidental counterpart to CXB296), together with CX863 appear consistent with the Sagittarius Arm, while CX31, CXB9, and CXB306 appear to lie in the Scutum-Centaurus Arm.

6.2. CX4 (CXOGBS J173931.2–290952)

This X-ray source was previously detected by *ROSAT*/PSPC (Sidoli et al. 2001) who noted that the source coincides with the supernova remnant G359.1+0.9 (Gray 1994). With a better position, we find that the *Chandra* source is inside the remnant, but off-center, but is a very close match to HD 316072. It was also serendipitously observed by *XMM-Newton*, and Farrell et al. (2010) note that the X-ray spectrum is consistent with thermal plasma. This, together with the close association with HD 316072 supports interpretation of the X-ray source as stellar coronal emission from this star, rather than being associated with the supernova remnant. The X-ray to bolometric flux ratio is unusually high for a late-type giant ($\log(F_{\text{X}}/F_{\text{bol}}) = -3.8$), as is the inferred X-ray luminosity, $L_{\text{X}} \simeq 3 \times 10^{31} \text{ erg s}^{-1}$, but it is near the

Table 4
Distances and luminosities based on Hipparcos parallaxes

| GBS | Spectral Type | $E(B - V)$ | Parallax (mas) | Distance (pc) | L_X (erg s^{-1}) | Comments |
|------|---------------|------------------|-------------------|--------------------|------------------------------------|-------------------------------|
| 26 | G3 V | -0.01 ± 0.03 | 9.35 ± 1.21 | 107 ± 14 | $(2.5 \pm 0.7) \times 10^{29}$ | ... |
| 53 | (F5 V) | -0.06 ± 0.04 | 9.74 ± 1.15 | 103 ± 12 | $(1.4 \pm 0.3) \times 10^{29}$ | Companion |
| 156 | (F0 V) | -0.04 ± 0.03 | 10.42 ± 1.10 | 96 ± 10 | $(3.8 \pm 0.8) \times 10^{29}$ | Coincidence or companion |
| 205 | F2 V | -0.03 ± 0.04 | 20.18 ± 0.59 | 49.6 ± 1.5 | $(1.2 \pm 0.1) \times 10^{28}$ | ... |
| 275 | F0 V | 0.04 ± 0.03 | 6.15 ± 0.78 | 163 ± 21 | $(1.1 \pm 0.3) \times 10^{29}$ | ... |
| 785 | F3 V | 0.01 ± 0.05 | 7.24 ± 1.45 | 138 ± 28 | $(3.5 \pm 1.4) \times 10^{28}$ | ... |
| B93 | M3 V | 0.00 ± 0.05 | 68 ± 45 | 15_{-6}^{+28} | $(8_{-5}^{+60}) \times 10^{26}$ | Color from Koen et al. (2010) |
| B422 | F2 | 0.08 ± 0.05 | 3.87 ± 1.56 | 260_{-70}^{+170} | $(1.0_{-0.5}^{+6}) \times 10^{29}$ | ... |

Table 5
Distances and luminosities based on spectroscopic parallaxes

| GBS | Spectral Type | Inferred $E(B - V)$ | Line-of-Sight $E(B - V)$ | Distance ^a (pc) | L_X ^a (erg s^{-1}) | Comments |
|------|---------------|------------------------|-----------------------------|-------------------------------|---|-----------------------------|
| 4 | G9 III | 0.23 ± 0.08 | 2.59 ± 0.28 | 470 | 3×10^{31} | ... |
| 6 | B0.5 III–Ve | 0.61 ± 0.03 | 2.16 ± 0.28 | 1100 | 2×10^{32} | B0.5 Ve assumed |
| 7 | K0 V | 0.07 ± 0.20 | 1.95 ± 0.28 | 100 | 7×10^{29} | ... |
| 9 | A5 | 0.17 ± 0.14 | 1.60 ± 0.22 | 600 | 3×10^{31} | A5 V assumed |
| 10 | G7 V | 0.37 ± 0.08 | 1.71 ± 0.25 | 51 | 2×10^{29} | RAVE spectral type |
| 12 | G5 | 0.41 ± 0.05^b | 3.63 ± 0.33 | 41 | 1.3×10^{29} | G5 V assumed |
| 31 | O9 V | 0.78 ± 0.05 | 1.89 ± 0.24 | 2600 | 4×10^{32} | ... |
| 33 | B0 Ve | 0.80 ± 0.04 | 2.65 ± 0.28 | 1300 | 8×10^{31} | ... |
| 72 | F8 | -0.16 ± 0.09 | 2.86 ± 0.41 | 180 | 3×10^{29} | ... |
| 77 | (B8 V) | 0.22 ± 0.04 | 1.54 ± 0.24 | 450 | 3×10^{30} | Coincidence |
| 91 | F8 | -0.06 ± 0.07 | 2.78 ± 0.42 | 200 | 3×10^{29} | Resolved binary |
| 115 | A2 + G7 IV | 0.31 ± 0.05 | 2.39 ± 0.26 | 350 | 1.4×10^{30} | Algol |
| 183 | A2 V | 0.13 ± 0.04 | 2.35 ± 0.31 | 210 | 1.9×10^{30} | ... |
| 256 | K0 III | 0.07 ± 0.06 | 1.19 ± 0.22 | 240 | 2×10^{29} | ... |
| 296 | F0 | -0.21 ± 0.30 | 1.86 ± 0.27 | 700 | 1.7×10^{30} | F0 V assumed |
| 333 | A4 III | 0.30 ± 0.05 | 1.67 ± 0.21 | 420 | 9×10^{29} | ... |
| 337 | A0 | 0.25 ± 0.09 | 1.57 ± 0.24 | 730 | 3×10^{30} | A0 V assumed |
| 402 | G5 | 0.23 ± 0.07^b | 1.79 ± 0.29 | 70 | 2×10^{28} | G5 V assumed |
| 485 | F8 | 0.07 ± 0.08 | 1.84 ± 0.23 | 170 | 8×10^{28} | F8 V assumed |
| 506 | A2/3 III | 0.34 ± 0.06 | 1.98 ± 0.25 | 370 | 4×10^{30} | ... |
| 514 | B9 | 0.08 ± 0.05 | 2.27 ± 0.31 | 720 | 1.3×10^{30} | B9 V assumed |
| 632 | K1 III | 0.34 ± 0.11 | 1.37 ± 0.23 | 390 | 5×10^{29} | RAVE spectral type |
| 863 | B3–5 Ia/b–II | 0.36 ± 0.04 | 1.39 ± 0.23 | 1300 | 5×10^{30} | B3 II assumed |
| 916 | F0 | 0.02 ± 0.06 | 1.78 ± 0.29 | 270 | 1.0×10^{29} | F0 V assumed |
| B5 | K5 | -0.03 ± 0.16^b | 1.70 ± 0.36 | 500 | 1.0×10^{31} | K5 III assumed |
| B9 | O8 III | 0.44 ± 0.02 | 2.43 ± 0.29 | 2700 | 3×10^{32} | ... |
| B17 | (F8) | 0.00 ± 0.12 | 0.90 ± 0.21 | 200 | 5×10^{29} | F8 V assumed; Coincidence |
| B116 | A5 | 0.21 ± 0.05 | 2.06 ± 0.34 | 340 | 4×10^{29} | A5 V assumed |
| B181 | A0 | 0.85 ± 0.09 | 1.18 ± 0.23 | 200 | 2×10^{29} | A0 V assumed |
| B211 | B9 III | 0.15 ± 0.04 | 3.13 ± 0.37 | 330 | 3×10^{29} | ... |
| B233 | A0 | 0.00 ± 0.07 | 1.31 ± 0.25 | 760 | 9×10^{29} | A0 V assumed |
| B287 | A2 IV/V | 0.22 ± 0.04 | 1.64 ± 0.28 | 340 | 2×10^{29} | ... |
| B296 | (B5/7 II/III) | 0.26 ± 0.06 | 2.67 ± 0.35 | 1100 | 2×10^{30} | B6 III assumed; Coincidence |
| B306 | B1 I–II | 0.49 ± 0.04 | 1.17 ± 0.22 | 2800 | 2×10^{31} | B1 II assumed |

^a We have not assessed uncertainties in distance or X-ray luminosity for these sources as we cannot reliably quantify uncertainties in the absolute magnitude.

^b For G and later spectral types, the intrinsic color is quite sensitive to the assumed luminosity class, so $E(B - V)$ is unreliable where this is not known.

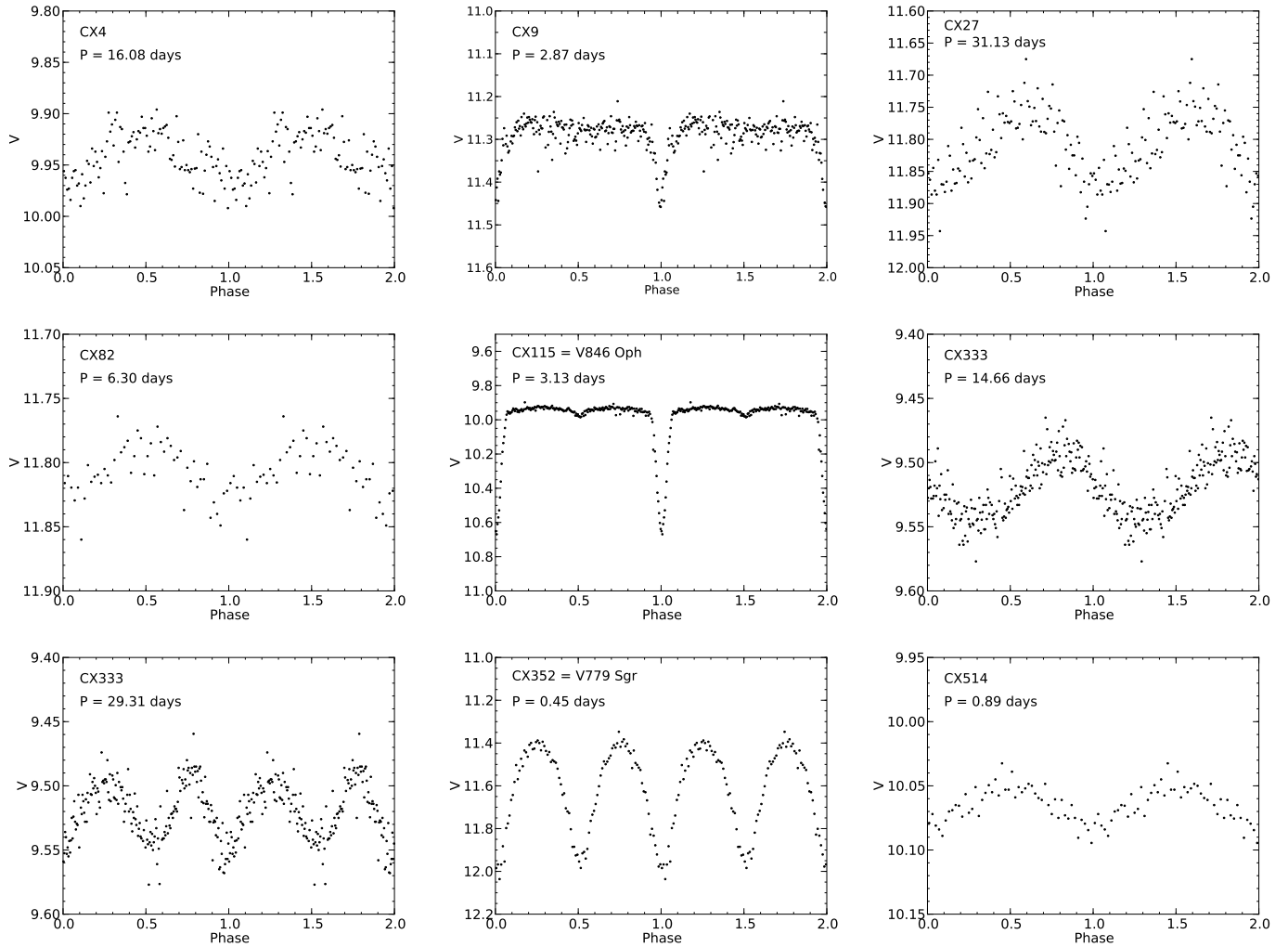


Figure 8. ASAS lightcurves of stars with identifiable periods. Note that CX4 also shows aperiodic long-term variability (Fig. 10), and that CX333 is shown twice with different periods.

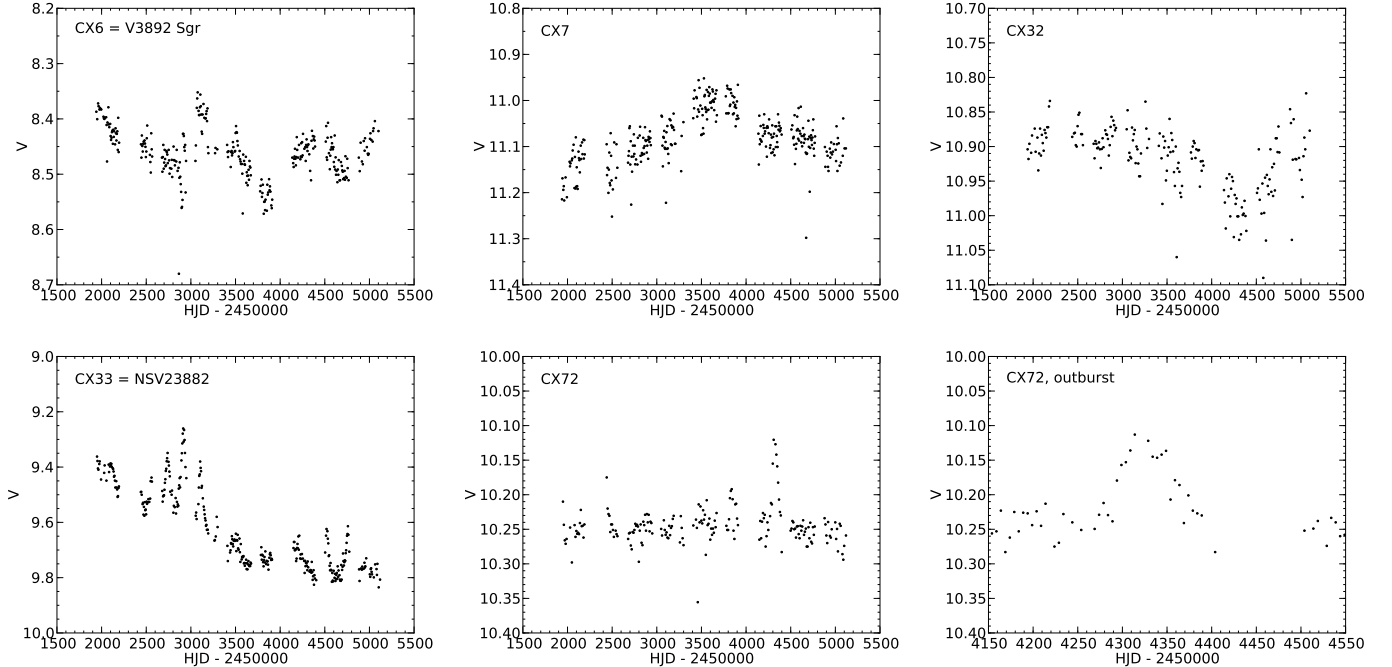


Figure 9. ASAS lightcurves of stars showing definite aperiodic variability. Note that CX72 is shown twice, the second as a close-up of the flare.

top of the range observed in other late-G giants, rather than outside it (Gondoin 2005).

HD 316072 is identified as a variable in ASAS data (Pojmanski 2002), strengthening the likelihood of it being the true counterpart further. A Lomb-Scargle periodogram yields a single clear period of 16.0811 ± 0.0026 days, with the uncertainty estimated by the bootstrap method. The periodicity has an amplitude of about 0.1 mag, is apparent in individual data points as well as in phase-binned data, and is present in multiple independent subsets of the lightcurve. We show the folded lightcurve in Fig. 8. The rotation rate is quite rapid for a giant, so there is no need to look for X-rays from a companion star and we can comfortably attribute the X-rays to coronal activity in the giant.

6.3. CX6 (CXOGBS J174445.7-271344)

HD 161103 is one of the prototypical Be stars identified as a class by Merrill et al. (1925). Early classifications include B2 III–V (Hiltner 1956) and B1 III (Garrison et al. 1977). Recent works favor a B0.5 III–Ve star (Steele et al. 1999; Lopes de Oliveira et al. 2006). As expected for a Be system, it shows a pronounced infrared excess over the colors expected for an isolated star due to the presence of circumstellar material and is also a strong outlier in $(J - H)$ vs. $(H - K)$.

This object is a long-known variable star, V3892 Sgr, and confirmed as a variable by ASAS (Pojmanski 2002). We show its lightcurve in Fig. 9. It exhibits relatively low amplitude irregular variations, at least by comparison with the other Be star in our sample, CX33.

HD 161103 emerged as a possibly more interesting object when Motch et al. (1997) matched it with a *ROSAT* source and inferred an unusually high luminosity for its spectral type (unabsorbed $L_x \simeq 10^{32}$ ergs $^{-1}$), and a quite hard color. Both characteristics stand out in our *Chandra* data as well. Based on these characteristics,

Motch et al. (1997) identified this as a candidate X-ray binary. Since the X-ray luminosity is lower than known Be + neutron star systems, they suggested a white dwarf companion. Lopes de Oliveira et al. (2006) studied this object further, identifying it as one of a number of objects analogous to γ Cas. They reported a 3200 s pulsation, although it was unclear if this was truly a coherent pulsation from a rotating compact object, or a quasi-periodic oscillation as seen in γ Cas. The nature of this object, and of the γ Cas analogs in general, remains unknown (Motch et al. 2007).

6.4. CX7 (CXOGBS J173826.1-290149)

TYC 6839-513-1 was spectroscopically classified as a K0 V star by Torres et al. (2006). These authors measured a Li equivalent width of 80 mÅ, comparable to the lower end of the distribution seen in Pleiades stars of the same color, suggesting that this is a young object.

This star is not identified as a variable in the ASAS variability catalog, but on examination it does show quite large amplitude, very slow variability (Fig. 9). It also does appear to show periodic variability with a period around 3.5 days, although this is only apparent after examining yearly periodograms (Figure 11). A primary period around 3.5 ± 0.1 days is apparent on most years, although the frequency is not stable, and sometimes two periods are seen. The quoted uncertainty primarily reflects the variations seen in the dominant period. In addition on a few years there is significant power at the first harmonic. Together, these frequencies and their aliases account for all the features seen in the periodograms. We interpret this behavior as variations caused by starspots that form at different latitudes subject to different rotation rates. Sometimes multiple spots may result in significant power at harmonics.

The X-ray to bolometric flux ratio of CX7 is very high, $\log(F_X/F_{bol}) = -3.33$ (Fig. 4), close to the limit of coro-

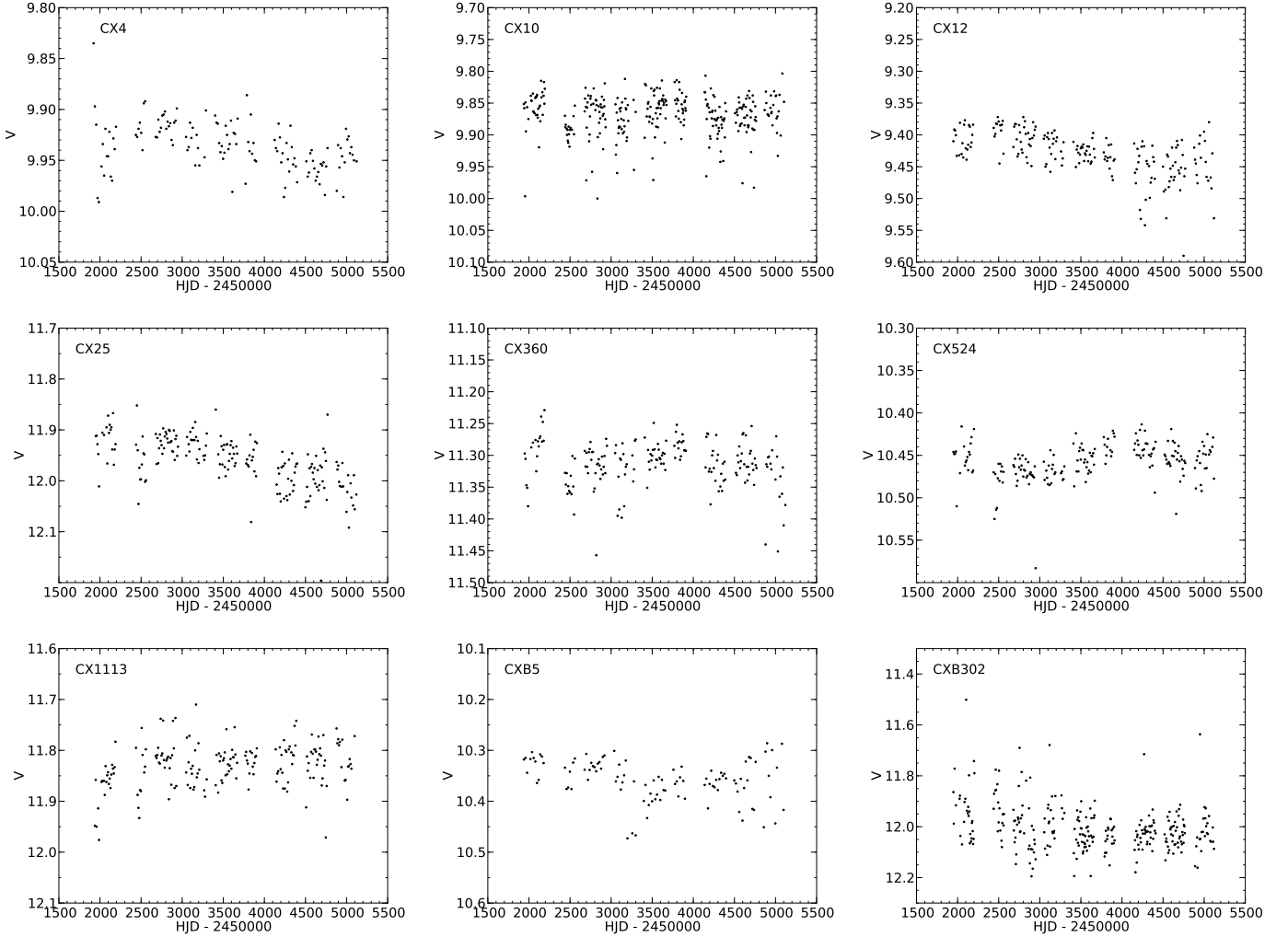


Figure 10. ASAS lightcurves of stars showing probable aperiodic variability. Note that CX4 also shows a periodic modulation shown in Fig. 8.

nal saturation, and together with CX9, it also stands out in X-ray to optical flux ratio above all of the other 67 stars considered (Fig. 3). We can use the spectral type to derive a convective turnover time (Wright et al. 2011) and combine this with the rotation period to obtain the Rossby number, $R_0 = P_{\text{rot}}/\tau = 0.23$. Comparing this with Figure 2 of Wright et al. (2011) this is close to the saturated regime, consistent with the very high value of $\log(F_X/F_{\text{bol}})$. The strong aperiodic variability, quite rapid rotation, and the high level of X-ray activity all support the classification of this object as a young K star.

6.5. CX9 (CXOGBS J173508.3–292328)

Superficially, this object presents a challenge for interpretation as an A star with the highest X-ray to bolometric flux ratio in our sample. The spectrum is among the harder objects in the sample, so if it is a coronal spectrum it must be rather hot, above 10 MK, atypical of later A stars which can show low-luminosity cool coronal emission. We then expect this system to be a binary of some kind, with the X-rays attributed to a companion star. This is indeed the case. This is an ASAS variable, showing shallow eclipses with period 2.8723 days

(Otero et al. 2006), see Fig. 8. No secondary eclipse is seen, and the IR colors are clearly redder than expected for a single A star (Fig. 5), so the companion is a late-type star, and the X-rays can probably be attributed to coronal activity. With F_X/F_{Bol} so close to the saturation line at $\log(F_X/F_{\text{Bol}}) \sim -3$, however, the companion must itself be very close to saturation. For the companion to have an acceptable F_X/F_{Bol} ratio, it must have a bolometric luminosity close to the A star, and so must be larger, and hence an evolved star. This may then be an Algol system.

We attempt to fit the infrared excess more quantitatively with a simple model. We assume that the primary is an A5 main-sequence star (we will justify this assumption later), with appropriate absolute magnitude and colors, and then consider a range of late-type giant companions, with the radius and spectral type of the companion allowed to vary freely, along with the reddening. We find acceptable fits to the photometry for a wide range of companions of spectral type G6 or later. All solutions involve a companion under-luminous for a giant, so we classify the companion as a G6 or later sub-giant. Formally, the best fits are found for a K1 IV companion with radius around $4.5 R_{\odot}$, and with $E(B - V) \simeq 0.14$ (close

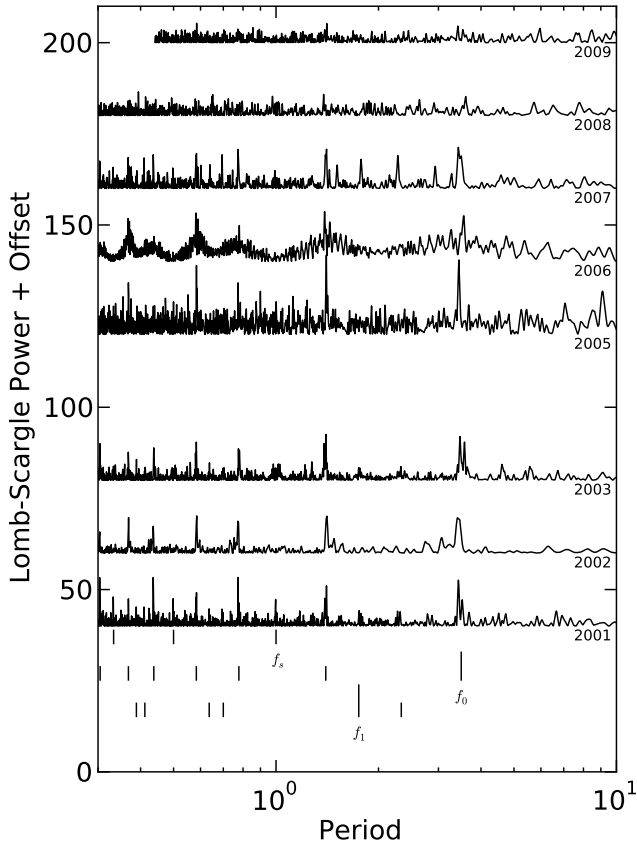


Figure 11. Yearly ASAS Lomb-Scargle periodograms for CX7. 2004 has been omitted as the sampling within this year compromised the periodogram. We label three sets of frequencies: f_s , the one-day sampling frequency and its harmonics; f_0 , the 3.5 day fundamental period and its aliases, and f_1 , the 1.75 day first harmonic and its aliases.

to that found above neglecting the companion). This is not a unique solution, but we will examine it further to show that it is consistent with other characteristics of the system. The K1 IV solution corresponds to a companion which is about 1 bolometric magnitude fainter, and the X-ray to bolometric ratio of the companion star alone then increases to $\log_{10}(F_X/F_{\text{bol}}) = -2.7$, placing the companion on or a little above the saturation line, but not implausibly so. With an A5/K1 binary, the ratio of V band surface brightnesses is about 30:1, so the companion star is too dim for a secondary eclipse to be seen, consistent with the lightcurve (Fig. 8). Finally, we can estimate the binary size given a 2.87 hr period and plausible masses. For a $\sim 2 M_{\odot}$ A5 V primary, the expected binary separation is then $a = 10.6(1 + q)^{\frac{1}{3}} R_{\odot}$. This is quite consistent with the inferred companion radius; for example if we assume $M_2 = 1.0 M_{\odot}$, then we expect its Roche lobe to have radius $3.9 R_{\odot}$, certainly consistent within the uncertainties on our crude estimates above. We note that if the A5 star were larger than a main-sequence star, then the companion would also have to be larger, and would not fit within the binary; the assumption of a main-sequence primary made above is thus justified.

We conclude that the properties of CX9 can be well explained by an eclipsing binary with an A5 V primary and a late-type sub-giant companion (with K1 IV adopted as a representative example). The companion must be either filling its Roche lobe (and actively transferring mass) or very close to it. It will therefore be tidally-locked, explaining the very high level of coronal activity in this system, which is then either an Algol, possibly in a mass-transferring phase, or an Algol-like system.

6.6. CX10 (CXOGBS J173629.0-291028)

HD 315992 was initially classified as an F8 star of undetermined luminosity class (Nesterov et al. 1995). More recently, HD 315992 was included in the RAVE 3rd Data Release (Siebert et al. 2011) from which we obtain $T_{\text{eff}} = 5369 \text{ K}$ and $\log g = 4.18$, pointing instead to a mildly evolved G7 star. The location in the $(J - H)$ vs. $(H - K)$ diagram ($J - H = 0.50 \pm 0.04$, $H - K = 0.20 \pm 0.040$) also favors a later spectral type.

This appears to be a rather active star, with a high X-ray to optical flux ratio and quite hard X-ray spectrum. It appears to show irregular variability in ASAS data, although this is one of the more marginal variables in our sample (Fig. 10). There is no evidence for an IR excess, and it lies on the single-star line in Fig. 5. While we cannot draw a definite conclusion, CX10 appears consistent with an active single star with no evidence for binarity.

6.7. CX12 (CXOGBS J174347.2-314025)

HD 318207 is one of the stars that appears to have an infrared excess, and correcting for extinction will only make this more dramatic, so this is likely a binary with a later-type companion. The location in the $(J - H)$ vs. $(H - K)$ also suggests the presence of a companion cooler than G5. Like CX10, this object shows a high X-ray to optical flux ratio, and quite a hard X-ray spectrum. It appears to show slow long-term variability in ASAS data (Fig. 10). We tentatively classify this as a binary containing one or two active stars, although the activity may in this case be unrelated to the binarity as the luminosity is not outside the range expected for single stars.

6.8. CX25 (CXOGBS J174502.7-315934)

TYC 7381-792-1 shows no detectable period, but does appear to exhibit irregular variability in ASAS data. The colors are consistent with a single star, with the JHK colors suggesting an early K main-sequence or late G giant type. It has a high X-ray to optical flux ratio and quite hard spectrum (like CX10 and 12). It is likely an active single star or binary.

6.9. CX27 (CXOGBS J173652.8-284841)

TYC 6839-636-1 has the third highest X-ray to optical flux ratio in our sample. The JHK colors suggest a late spectral type, and are quite similar to CX4, possibly pointing to a giant. We identify this as a variable in ASAS data with a periodic modulation about 0.15 mag and period 31.13 days. The lightcurve is shown in Fig. 8. Combined with the colors, this period suggests this is an active late-type giant.

6.10. CX31 (CXOGBS J173803.5-290706)

CX31 is identified with LS 4306s, the southern object of a pair of O stars about 25 arcsec apart. It has an O9 V spectral type (Vijapurkar & Drilling 1993). We estimate $E(B - V) = 0.78 \pm 0.05$. Savage et al. (1985) included this star in a catalog of UV extinction determinations and estimate a slightly higher but roughly consistent $E(B - V) = 0.99$. Our distance estimate for $E(B - V) = 0.78$ is 2.6 kpc, consistent with Savage et al. (1985), with a height above the plane of about 80 pc.

The relatively high luminosity, coupled with an unusually hard X-ray spectrum for a massive star flag this as an unusual object. The inferred interstellar reddening is higher than for the other OB stars in the sample, but not outside the range considered in Section 5, so if there is no additional absorption, the X-ray colors favor temperatures above 40 MK. Local absorption is not generally seen in O stars, where the X-rays are believed to originate sufficiently far from the stellar surface to not be seen through a large column. If there is substantial local absorption, then the unabsorbed X-ray luminosity, and hence the F_X/F_{bol} ratio, become even larger.

This object does appear in the Washington Double Star Catalog (Mason et al. 2001). The companion star is about 2 arcsec away, corresponding to about 5000 AU at 2.6 kpc, making this an extremely wide binary if it is indeed a physical association. The companion is 3.5 mag fainter than the O star, so if it is a main-sequence star, would be have a spectral type around B5. The X-rays clearly originate from the O star, however, and not from the companion or a point in between, and it is unlikely that the presence of the companion is pertinent to the origin of the X-rays.

It remains possible that the O star itself is a much closer inner binary. In the optical/IR color-color plot it lies on the single star track, but that could only indicate two stars of similar spectral type. In this case, the unusual X-ray emission could indicate this is a colliding wind system. A compact companion is also a possibility, which would make this a quite low luminosity X-ray binary.

6.11. CX32 (CXOGBS J174104.9-281503)

We find TYC 6839-218-1 to be variable in ASAS data with slow, and probably irregular variations of about 0.1 mag. Its X-ray to optical flux ratio, and X-ray color are both unremarkable for stellar X-ray emission. The *JHK* colors are consistent with a G or K star.

6.12. CX33 (CXOGBS J174835.5-295728)

HD 316341 is a known Be star, although rather less well studied than HD 161103 (CX6) and has never been proposed to be a Be X-ray binary. Like CX6, and as expected for a Be system, it shows a pronounced infrared excess over the colors expected for an isolated star due to the presence of circumstellar material, and is an outlier in $(J - H)$ vs. $(H - K)$. It is also a known variable, NSV 23882, and was clearly identified as variable by ASAS. Its lightcurve is shown in Fig. 9. There is substantial variability, both an overall decline and several outbursts, with an overall range of around 0.5 mag. The outbursts appear to have a characteristic recurrence time of about 200 days, but are not strictly periodic and outburst separations range from 180–230 days. CX230

appears to be an off-axis detection of this object, indicating that substantial X-ray variability is also present, since this corresponds to a $4\times$ fainter X-ray flux than its detection as CX33.

Beyond being a Be star, it is unclear how to classify this. The X-ray luminosity is not remarkable for single Be stars, especially not B0 stars, and is lower than the typical range for γ Cas stars (Motch et al. 2007). The spectrum is harder than is typical, however, with a hardness ratio comparable to the γ Cas analog, CX6. As a B0 star, it also lies very close to the narrow range of spectral types around B0.5 seen in the other γ Cas analogs. It may be a lower luminosity member of the class, or one temporarily caught in a low-luminosity state.

6.13. CX53 (CXOGBS J174448.8-263523)

CX53 was matched against HD 161117, although with a quite large offset of 3.33 arcsec. Initially we flagged this object as a possible chance alignment. HD 161117 is a resolved double star, however, with a 12th magnitude companion listed in the Tycho Double Star Catalog (Fabricius et al. 2002). Using the coordinates and proper motions of this star we find an offset of 0.52 arcsec from the *Chandra* position at the epoch of the *Chandra* observations, so we believe this is likely to be the true counterpart to the X-ray source. If it is a true binary, then the reddening, distance, and X-ray luminosity will be the same as calculated in Table 4. This double is also listed in the Washington Double Star Catalog (Mason et al. 2001). The two stars have very similar proper motions, with a common proper motion of 46 mas yr^{-1} , and a difference between them of just 7 mas yr^{-1} . The latter is approximately consistent with the orbital proper motion expected for a binary star separated by about 3 arcsec at 100 pc, so we believe this is indeed a true binary.

The companion is 3.4 mag fainter than HD 161117, but otherwise no information is known about it. If it is a main-sequence star, then we expect a spectral type around K4 V. Associating this star with the X-ray source implies a true $\log(F_X/F_{\text{opt}}) = -2.52$, placing it among the X-ray brighter objects in our sample. The X-ray hardness, however, is unremarkable for coronal emission from late-type stars.

6.14. CX59 (CXOGBS J174500.5-261228)

CX59 was matched with TYC 6832-663-1 with a quite large offset of 3.53 arcsec. This source was detected only 3 arcmin off-axis by *Chandra* with 27 photons, so there is no reason to expect such a large offset. This star has not been reported as a double, and the X-ray source is also the hardest of the sources considered here for which we can calculate a hardness ratio. We conclude that this is likely to be a chance alignment.

6.15. CX72 (CXOGBS J174820.3-302836)

The X-ray spectrum of CX72 is quite soft, consistent with coronal emission. The object lies above the line in the IR/optical color-color diagram (Fig. 5), with a significant IR excess relative to its Tycho-2 color. In general this indicates a cooler companion, but in this case, the *JHK* colors are consistent with its F8 spectral type, with moderate reddening, so the Tycho-2 color may be at fault, leaving no convincing evidence for a cool companion.

We identified an outburst in the ASAS lightcurve of HD 316356 (Fig. 10). This is quite significant with amplitude 0.15 mag and lasting for three months. The outburst behavior is quite different to the flares of coronally active stars and requires a different explanation further arguing against associating the X-rays with a cool, active companion. The outburst itself is more reminiscent of dwarf nova outbursts in morphology, although the duration is substantially longer than typical dwarf nova outbursts. Aside from the outburst, HD 316356 shows no significant variability in the ASAS data, and in particular no evidence for ellipsoidal variations as would be expected if it were the donor star in a cataclysmic variable. A chance alignment with an unrelated dwarf nova, or a hierarchical triple cannot be ruled out, but it would then be a quite improbable coincidence with a quite atypical dwarf nova, so this seems unlikely. At this point, the nature of the outburst remains unclear.

6.16. *CX77 (CXOGBS J173638.3-285945)*

CX77 lies close to TYC 6839-487-1, although with a 6.32 arcsec offset this is likely to be a chance alignment. This star is also HD 159571 (Fabricius et al. 2002), although we note that the SIMBAD coordinates listed for HD 159571 lie rather far from TYC 6839-487-1 and do not appear to coincide with a bright star at all.

As for CX53, this star is listed as a double (Fabricius et al. 2002). Both stars have astrometry included in the UCAC-3 catalog (Zacharias et al. 2010), although the proper motions for the companion star are flagged as suspect. The offset of the companion star from the X-ray source is 1.17 arcsec. The companion star has been detected by both 2MASS and the *Spitzer* GLIMPSE Point Source Catalog¹¹. The colors from J to $8\mu\text{m}$ are flat, and difficult to reconcile with a cool star. The colors and apparent magnitude are as would be expected for an A star at around the distance of HD 159571. The X-ray source itself is strongly variable, being not detected in an observation closer to on-axis, and is rather hard, and neither these characteristics, nor the inferred luminosity, would be typical for an A star. It seems quite likely it is indeed an unrelated object and that this object should be classified as a chance coincidence.

6.17. *CX82 (CXOGBS J175709.5-272532)*

CX82 is matched with TYC 6849-1294-1. There is very little information about this star and no published spectral type. The Tycho-2 colors are consistent with a G type star or earlier, but have large uncertainties so a cooler star cannot be ruled out. The colors lie above the single-star line in Fig. 5, but the $(B - V)$ color is too uncertain to say this with confidence. The JHK colors favor a K3-5 classification, with a $V - K$ color also consistent with this.

We find this object to be variable in ASAS data with a 6.3 day period and 0.1 mag amplitude (Fig. 8). The X-ray to optical flux ratio is among the highest objects in the sample. Both characteristics would point to a rapidly rotating active star or binary. Combining the 6.3 day period with a possible spectral type around K4, we would expect a Rossby number of $R_0 \sim 0.29$ (see Section 6.4), consistent with a star near coronal saturation.

¹¹ <http://irsa.ipac.caltech.edu/data/SPITZER/GLIMPSE>

6.18. *CX91 (CXOGBS J175610.9-271426)*

HD 314883 shows no peculiarities in our data, with no variability and an insignificant deviation from the single-star line in Fig. 5. It is however a noted (close) resolved binary (see e.g. Fabricius et al. 2002). The two components are separated by 0.87 arcsec with both consistent with the X-ray position to within an arcsecond. They appear to share common proper motion, and have very similar V_T and B_T magnitudes. This appears to be a real binary with two very similar stars. The X-rays could originate from either component, or from a combination of the two. The X-ray to optical flux ratio is unremarkable for one, or two, late F stars, and so most probably reflects normal coronal emission.

6.19. *CX115 (CXOGBS J173940.8-285111)*

CX115 is clearly the X-ray counterpart to V846 Oph (HD 316070), a known eclipsing Algol system. Budding et al. (2004) list this object as having an A2 primary and G7IV secondary star. Their fits to the lightcurve give mass ratio $q = 0.15$, $i = 78^\circ$, and a reasonable likelihood that this is a semi-detached system.

CX115 is one of the objects showing a pronounced infrared excess (Fig. 5) relative to single stars. If we assuming an A2 primary and G7IV secondary as above, we estimate that the companion contributes about 15-20% of the light in the V band and has a negligible effect on the reddening estimate, so the distance estimate above should be increased by only about 10%. For comparison, Singh et al. (1996) cite a distance of 580 pc, and a *ROSAT*/PSPC X-ray luminosity of $6 \times 10^{30} \text{ erg s}^{-1}$.

The eclipses are very clearly seen in the ASAS data, although it is surprisingly omitted from the catalog of variables. We show the folded lightcurve in Fig. 8. The period we derive from this photometry is 3.12678 ± 0.00014 days, in perfect agreement with the period of 3.1268 days cited by Budding et al. (2004). The secondary eclipse is small, but detectable, and the lightcurve shows additional variability out of eclipse.

6.20. *CX156 (CXOGBS J174928.3-291859)*

CX156 appears to be a chance alignment with HD 161907, with an offset of over 6 arcsec. The most likely match to the X-ray source is 2MASS J17492831-2918593, located just 0.09 arcsec from the X-ray position. The colors ($J - K = 0.65 \pm 0.11$) would suggest an early-K spectral type. At $K = 9.30$, this star would then be about the right brightness for an early K main-sequence star at a distance of 100 pc. It is therefore possible there is a physical association of this star with CX156, although the only evidence in favor of this is that they plausibly lie at the same distance.

6.21. *CX183 (CXOGBS J175041.1-291644)*

HD 162120 lies off the single-star track in Fig. 5, although it is not one of the most significant IR excess cases. It shows no apparent variability or other peculiarities. It probably has a late-type companion star contributing the X-ray emission, although there is no evidence for or against identifying this as a close Algol-like system.

6.22. CX205 (CXOGBS J174917.2–303551)

HD 161852 is the brightest star in the sample, and saturated in ASAS data. This is classified as an F2IV/V star (Houk 1982). The optical brightness would suggest a main-sequence rather than sub-giant classification at the *Hipparcos* distance of 50 pc.

HD 161852 was included in the X-ray survey of *Hipparcos* F stars using *ROSAT* by Suchkov et al. (2003). The *ROSAT* estimate of the X-ray luminosity of 7.6×10^{28} ergs $^{-1}$ is in a softer band than our *Chandra* observation. It was found to be a little below average for F stars of approximately Solar metallicity as this is ($[\text{Fe}/\text{H}] = -0.1$), and indeed this is among the lowest F_X/F_{bol} objects in our sample.

6.23. CX256 (CXOGBS J175348.1–284118)

With $\log(F_X/F_{\text{bol}}) = -5.9$, HD 162761 is quite typical of single K0III stars ($\log(F_X/F_{\text{bol}}) = -5.6 \pm 0.5$; Hünsch et al. 1998). Richichi et al. (2008) observed a Lunar occultation of this object, and identified a companion 0.11 arcsec away, with a brightness ratio of approximately 1:120 relative to the giant. If this is a physical binary, the separation at 240 pc would be about 25 AU. A K0 main sequence companion star would be consistent with the brightness ratio, but would then have an X-ray to bolometric flux ratio of around 10^{-4} , possible, but amongst the most active late-type stars in our sample. Identifying the X-rays with the visible giant star is more plausible.

6.24. CX275 (CXOGBS J174205.3–265046)

CX275 lies about 2 arcsec away from HD 160627. While the offset is quite large, this was observed at quite a large off-axis angle, and the offset is consistent with the X-ray positional uncertainty (Jonker et al. 2011). The X-ray luminosity is quite high for an F0 V star. HD 160627 is quite rapidly rotating, however ($v \sin i \simeq 30$ km s $^{-1}$; Nordstrom et al. 1997), and the X-ray luminosity is consistent with other F dwarfs with similar rotation (Maggio et al. 1987).

6.25. CX296 (CXOGBS J174951.1–295611)

HD 316432 is a very good positional match to CX296. It lies above the single-star line in Fig. 5, however the uncertainty in its Tycho-2 color is large, and the Tycho-2 color is bluer than an F0 star should be. If we instead assume a typical F0 color (consistent within uncertainties), then there is no significant IR excess. The only real peculiarity about this object is the high implied X-ray luminosity, and the high F_X/F_{bol} . This suggests an unusually active F star, possibly a binary, although there is no detected variability to support this classification.

6.26. CX333 (CXOGBS J173617.5–283417)

HD 159509 is a resolved double (Fabricius et al. 2002), with the companion lying closer to the X-ray position, so it is possible that HD 159509 is not the true counterpart. This was observed far enough off-axis that neither star can be ruled out with confidence. The brighter star is a suspected variable (NSV 22873; Samus et al. 2009). The ASAS data confirm a clear modulation with period of 14.6565 days, or more likely twice that with ellipsoidal variations (Fig. 8). The optical/IR colors, too,

indicate that this is not a single A-type giant as there is a clear infrared excess, corresponding to IR magnitudes about 1 mag brighter than expected for the A star. Together, these facts would suggest that HD 159509 has a late-type companion. Since an A3/5 III star should be about ten times too small to fill its Roche lobe in a 30 day binary, it may be that the (low-amplitude) ellipsoidal variations actually arise from the small contribution to the visible light from a larger late-type giant companion. This would make this another Algol-like system with an evolved late-type companion to an A star, although in this case a giant. Fixing the primary to A4 III, we find a best fit to the *BVJK* photometry for a K1 IV/III companion. Given that it appears to be an Algol-like system, it seems natural to associate the X-rays with HD 159509 rather than the slightly closer alternate star. There are comparable Algol systems. For example, RZ Cas has a 32.3 day period, an A5 IIIe primary, and K1 III secondary (Malkov et al. 2006).

6.27. CX337 (CXOGBS J173527.2–293046)

CX337 also matches an A star, HD 315995. Like many of the A stars in our sample, this shows colors inconsistent with a single star (Fig. 5) indicating the presence of a cooler companion. If we assume a main-sequence primary, we can fit the *BVJK* photometry well for a range of late-G to early K sub-giant companions, much as for the other A stars in the sample.

6.28. CX352 (CXOGBS J175537.1–281759)

CX352 clearly coincides with the contact binary, V779 Sgr (HD 316675). Its spectral type in the Henry Draper Charts is listed as F8 (Nesterov et al. 1995), with the companion inferred to be F9 (Svechnikov & Kuznetsova 2004). Its Tycho-2 color is anomalous, presumably due to the large amplitude variability, so we can make no reddening estimate.

V779 Sgr is included in the ASAS Catalog of Variable Stars. A Lomb-Scargle periodogram gives a very sharp peak at 0.222515 days. This is the first harmonic as dominates in all ellipsoidal variables, and the orbital period is twice this, $0.44503040 \pm 0.00000018$ days, with a bootstrap uncertainty. The folded lightcurve is shown in Fig. 8, and shows a modulation amplitude of about 0.6 mag.

Estimates of system parameters are presented by Branczewicz & Dworak (1980), who attribute 56% of the light to the brighter component, which has a radius $1.48 R_{\odot}$. Svechnikov & Kuznetsova (2004) alternatively attribute the brighter component 70% of the light, and radius $1.44 R_{\odot}$. We then expect an absolute magnitude about 1 mag brighter than a single F8 star if the light from both stars is included. At maximum light, when we see both stars well, it is observed by ASAS to be around $V \simeq 11.4$, so allowing for the light from both stars, we estimate a distance around 500 pc, neglecting the unknown extinction. This would correspond to $L_X \simeq 7 \times 10^{29}$ ergs $^{-1}$.

6.29. CX360 (CXOGBS J175114.4–291912)

CX360 lies 4.07 arcsec from TYC 6840-525-1. CX191 also appears to be an off-axis detection of this source. CX360 was observed at only 2.8 arcmin off-axis, so there

is no reason to expect such a large positional error and this star is almost certainly not the true counterpart. It is not noted as a double, so this is likely a chance alignment with an unrelated object. We note that TYC 6840-525-1 does appear to show irregular variability in the ASAS lightcurve (Fig. 10), although it is one of the weaker detections in our sample.

6.30. *CX388 (CXOGBS J173659.3-290603)*

CX388 lies 4.79 arcsec from TYC 68390615-1. This was observed at only 0.9 arcmin off-axis, so the positional offset is highly significant and this star is almost certainly not the true counterpart. It is not noted as a double so, again, this is likely a chance alignment with an unrelated object.

6.31. *CX402 (CXOGBS J173533.2-302336)*

The optical counterpart to CX402 appears to be the G5 star HD 316033. The activity level is not atypical for G dwarfs, but the optical/IR colors would suggest the presence of a cooler companion as well, although this is not one of the more significant IR excesses in our sample.

6.32. *CX485 (CXOGBS J173718.7-282925)*

The optical counterpart to CX485 appears to be the F8 star HD 316059. This object shows pronouncedly redder IR than optical colors, indicating the presence of a cooler companion. The X-rays can most likely be attributed to coronal activity from one or both of the stars.

6.33. *CX506 (CXOGBS J174045.9-280148)*

CX506 is well aligned with HD 160390. This star actually lies rather close to the single-star line in Fig. 5, unlike most of the A stars in our sample. A small IR excess may be present, but we find by fitting the *BVJK* colors that this is only sufficient to accommodate a late-type main-sequence or slightly evolved star, no more than a magnitude above the main-sequence. Late-type giant, and probably sub-giant companions can probably be ruled out. The allowed companions (later than F0) all have bolometric magnitudes at least 3.2 mags fainter than the A giant, and so if we attribute the X-rays to the (putative) companion, they would have $F_X/F_{\text{bol}} \gtrsim -3.5$, so would be close to coronal saturation and very active. Such a case cannot be ruled out, but we should stress that there is no evidence (other than the presence of X-ray emission) for such a companion.

6.34. *CX514 (CXOGBS J175637.0-271145)*

CX514 lies near the B9 star HD 314884. With an X-ray luminosity of at least $10^{30} \text{ erg s}^{-1}$, and $F_X/F_{\text{bol}} = -5.4$, this falls well outside the norms for late B stars, so either this is a chance alignment, or a companion is present.

We do find HD 314884 to be variable in ASAS data, showing a 0.89 day period (Fig. 8). The periodicity is stable in amplitude and phase through the period covered by ASAS. Besides variability and X-ray emission, there is no other evidence for multiplicity in this system. The optical/IR colors are consistent with a single B9 star, ruling out late-type sub-giant or giant companions (if the primary is main-sequence), but a main-sequence companion could still be present, or an evolved companion to a B giant. If the putative companion is an early K

or earlier type then the X-ray emission can be accounted for with $\log(F_X/F_{\text{bol}}) < -3$. Such a companion would have to be quite active, but this is expected since it would also have to be quite young if in a binary with a B9 star.

6.35. *CX524 (CXOGBS J175419.3-283654)*

TYC 6853-80-1 appears to be an irregular variable in ASAS data (Fig. 10). Its *JHK* colors favor a K star, or possibly a G giant like CX4. This then appears to be a late-type, somewhat active star.

6.36. *CX622 (CXOGBS J173654.1-295231)*

CX622 is offset 2.37 arcsec from TYC 6839-19-1. This was observed at 3 arcmin off-axis, so we would not expect such a large error in the X-ray position. There is very little information available about TYC 6839-19-1 but it shows no peculiarities that would support identifying it as the true counterpart to the X-ray source. This then, is likely to be a chance alignment.

6.37. *CX632 (CXOGBS J173353.9-292355)*

CX632 lies 1.28 arcsec from HD 315998. This was originally classified as a K5 star (Nesterov et al. 1995). It is one of our stars that is included in the RAVE 3rd Data Release (Siebert et al. 2011) from which we obtain $T_{\text{eff}} = 4533 \text{ K}$ and $\log g = 2.08$. From this, it is clearly a giant and the temperature then indicates a spectral class around K1. Hence we classify this as K1 III. With $\log(F_X/F_{\text{bol}}) = -5.6$, the X-ray emission is quite typical of single K1 III stars for which Hünsch et al. (1998) find a distribution of ratios -5.5 ± 0.5 . The optical/IR colors are consistent with a single giant star.

6.38. *CX698 (CXOGBS J175220.8-290427)*

TYC 6853-1354-1 matches well with the position of CX698. The optical color would suggest a mid-F star or earlier, whereas the IR color is redder, possibly indicating the likely presence of a cooler companion, although the IR colors are flagged by 2MASS as suspect.

6.39. *CX785 (CXOGBS J174249.9-275038)*

CX785 coincides with HD 160769. This object falls above the single-star line in Fig. 5, but the 2MASS *J* and *H* photometry is flagged as suspect. The DENIS survey¹² is in reasonable agreement, with $J - K_S = 0.55 \pm 0.09$, so the IR excess in this object appears to be real indicating a cooler companion. We can find a reasonable fit to the *BVJK* photometry with a late-K companion star a little above the main-sequence. It is quite possible that this is the origin of the X-rays instead of the F3 star.

6.40. *CX863 (CXOGBS J173303.4-293902)*

The optical counterpart to CX863 is clearly HD158902. This is a mid-B supergiant, originally classified as B8 by Cannon & Pickering (1918-1924). More recent two-dimensional classifications from objective prism surveys have given spectral types of B5 Ia (MacConnell & Bidelman 1976), B5 Ib (Garrison et al. 1977), and B3 II (Houk 1982). The implied distance

¹² VizieR On-line Data Catalog: II/263

would then range from 1.3 kpc (B3 II) to 4.5 kpc (B5 Ia). Given that the GBS is observing out of the plane, and this source is at $b = +1.94^\circ$, less luminous stars seem most likely, since they imply shorter distances from the plane. For a distance of 1.3 kpc, the distance above the plane is about 70 pc, whereas for 4.5 kpc it is 160 pc. We therefore suggest this is a B3 II star at a distance of 1.3 kpc, although a more distant and more luminous object remains possible. The properties of this star are quite normal for its spectral type. Its F_X/F_{bol} ratio is quite reasonable, it shows no variability, and its optical/IR colors are close to the single star line. The IR colors are a little redder than expected but the deviation is not highly significant.

6.41. CX904 (CXOGBS J175625.3-271043)

CX904 is a good match to TYC 6849-1144-1. It does fall above the single-star line in Fig. 5 suggesting it may be a binary, but the IR excess is not significant without either a spectral type or a more reliable optical color. The *JHK* colors alone would suggest a K spectral type.

6.42. CX916 (CXOGBS J175543.3-280443) and CX917 (CXOGBS J175543.0-280446)

CX916 matches TYC 6849-227-1 (HD 316666A) within 0.69 arcsec. CX917 matches HD 316666B within 1.5 arcsec. HD 316666A does show something of an IR excess in Fig. 5, although it is not highly significant. It may itself be an unresolved binary. This was identified as a candidate variable by Piquard et al. (2001) with a period of 0.173946 days. We could not reproduce this, or any other periodicity in the ASAS data.

We have much less information on the companion. It is independently detected by 2MASS with $K = 9.878 \pm 0.033$, 1.17 mags fainter than HD 316666A. The difference in magnitudes would be appropriate for a G0 V star, and the *JHK* colors are consistent with such a classification.

6.43. CX1113 (CXOGBS J174011.4-280212)

CX1113 matches well with TYC 6835-312-1. This star shows marginal evidence for irregular variability and its *JHK* colors would suggest a G star, but we have no other constraining information.

6.44. CXB5

CXB5 coincides very closely to HD 315961, originally classified as a K5 star (Nesterov et al. 1995). Neese & Yoss (1988) instead classified this star (listed as PSD 157-562; Barbier-Brossat & Figon 2000) as K0 III, with $E(B - V) = 0.3$, and a distance of 504 pc, based on DDO photometry. Neese & Yoss (1988) compare their photometric classifications with those from objective prism spectroscopy, and find scatters of up to around five spectral subclasses, and two luminosity classes, so this should be considered rather uncertain. The quite high X-ray luminosity, $L_X \simeq 1.0 \times 10^{31} \text{ erg s}^{-1}$, together with a high $\log(F_X/F_{\text{bol}}) = -4.3$ (compared to 5.6 ± 0.5 ; Hünsch et al. 1998) points to a quite active giant.

We see no evidence for a periodicity in the ASAS data, but the star does seem to be an irregular variable (Fig. 10). The X-ray color is rather hard, comparable to other stars at high $\log(F_X/F_{\text{bol}})$ such as CX4, 10, and 12. It appears to be quite comparable to CX4 in some ways,

and that also shows irregular variability in addition to its periodicity.

This is noted as a double with a fainter, yet bluer companion 1.6 arcsec away (Fabricius et al. 2002). The X-rays are clearly associated with the K star, however, and it is unclear if the nearby star is physically associated.

6.45. CXB9

CXB9 is associated with HD 161853. This is clearly an OB star, but there is uncertainty about its classification. It was originally listed as B3 by Cannon & Pickering (1918-1924), and then revised to B0/1 II in the Michigan HD classification (Houk 1982). Other estimates have included O7.5 (Crampton 1971), O8 V ((n)) (Walborn 1973), O7.5 V n (Garrison et al. 1977), O9 I (Hu et al. 1993), and finally an O8 III post-AGB star (Parthasarathy et al. 2000) based on its association with IRAS 17460-3114. Suárez et al. (2006) instead argue that it is not a post-AGB star, but instead a young object.

Based on UV data, Savage et al. (1985) estimated $E(B - V) = 0.54$, in fair agreement with our estimate of $E(B - V) = 0.44 \pm 0.02$. The implied distance is then 2.7 kpc and the distance below the plane is about 70 pc (Straizys & Kuriliene 1981). This would be consistent with the Scutum-Centaurus Arm. Main sequence types would situate it closer to 2.0 kpc, between Scutum-Centaurus and Sagittarius, while a supergiant classification would put it at 4-6 kpc, consistent with either the Norma Arm or the 3 kpc Arm. In the latter cases, the distance below the plane is, however, larger, 110-190 pc. Overall, an O8 III star at around 2.7 kpc in the Scutum-Centaurus Arm appears to fit best. For this case, the X-ray luminosity is about $3 \times 10^{32} \text{ erg s}^{-1}$. This is quite high, but the F_X/F_{bol} ratio is not excessive, and with quite soft colors this appears consistent with normal emission for O star winds. There is no variability seen in this object, and no evidence of binarity is reported. While the optical/near-IR colors we examine here are normal for a single star, it does have an mid-IR excess (Clarke et al. 2005). As noted above, Suárez et al. (2006) suggest that this is evidence that it is a young object.

6.46. CXB17

CXB17 lies near the F8 star HD 316565 (Nesterov et al. 1995), but with an offset of 4.98 arcsec, this is likely to be a chance alignment. We note that a 2MASS J17543011-2923572 is coincident with the X-ray source and is a much more likely counterpart.

6.47. CXB93 and CXB36

CXB93 coincides with a nearby M dwarf, LTT 7072 = GJ 2130A = HD 318327A. It is one component of a 20 arcsec separation binary, with the companion GJ 2130B = HD 318327B also detected by the GBS as CXB36. The spectral type of GJ 2130A has been variously estimated as M0 (Nesterov et al. 1995), M1.5 (Bidelman 1985), M2 (Stephenson & Sanduleak 1975), and M3 (Raharto et al. 1984), with the order reflecting that the determinations, not of the publication. The same works cite spectral types of M2-5 for GJ 2130B. GJ 2130A appears above the single-star line in Fig. 5. In

this case, it appears to reflect the large uncertainty in the Tycho-2 $B - V$ color, or inaccuracy of the transformations from $B_T - V_T$ for very red objects. An independent estimate gives $B - V = 1.465$ (Koen et al. 2010), in better agreement with its spectral type.

The X-ray luminosity of GJ 2130A is actually rather low among M dwarfs, for which Schmitt et al. (1995) find a range from $10^{26} - 10^{29}$ erg s $^{-1}$. While there is uncertainty in the *Hipparcos* parallax distance, spectroscopic parallax distances favor short distances, and low luminosities as well, ranging from 16 pc for M0 to 12 pc for M3. Partly this discrepancy may reflect the softer bandpass used by *ROSAT*, with our *Chandra* observations possibly missing much of the X-ray flux. The companion, is X-ray brighter, with $L_X \simeq 1.5 \times 10^{27}$ erg s $^{-1}$.

Optically, GJ 2130A was studied by Rauscher & Marcy (2006) as part of a survey of chromospheric emission in late K and M dwarfs. It was found to show the strongest Ca II emission among stars of comparable absolute magnitude.

6.48. CXB211

CXB211 lies 2.61 arcsec from HD 160826, but this was observed at a large off-axis angle (8.6 arcmin), so this is still a plausible match. HD 160826 is classified as a B9 V star (Houk 1982), so should not be an X-ray source in its own right. This object shows no noticeable IR excess, but we do note this is a resolved double with a separation of 0.6 arcsec (Fabricius et al. 2002). The nearby star has $V = 10.15 \pm 0.04$ and $B - V = 0.43 \pm 0.05$, and lies at 2.90 arcsec from CXB211. If this is a physical binary with the same reddening and distance then this would be a late-F or early G giant or sub-giant. It is likely that this is the true X-ray counterpart rather than HD 160826 itself as both stars are consistent with the poorly constrained X-ray position.

6.49. CXB287

CXB287 lies 1.39 arcsec from HD 158982, but the offset is not significant as this was observed 5.9 arcmin off-axis. HD 158982 is classified as a A2 IV/V star by Houk (1982), so should not be an X-ray source. This is listed as a resolved double by Mason et al. (2001), with a separation 0.3 arcsec. The companion may be the true counterpart. It is only 0.4 mag fainter than the A2 star, so is also unlikely to be a significant X-ray source in its own right unless it is a cooler sub-giant or giant, rather than a main-sequence star of type A4 or so, or the companion is closer than the A star.

6.50. CXB296

CXB296 lies 5.95 arcsec from HD 161839, making this star itself inconsistent with the X-ray source given a modest off-axis angle (2.1 arcmin). This star was originally classified as B5, but the Michigan Catalog updates this to B5/7 II/III (Houk 1982). An alternative classification of B2 V was proposed by Garrison et al. (1977). All of these classifications would correspond to $E(B - V)$ between 0.25 and 0.35, and a range of distances of 1–5 kpc. HD 161839 has a pronounced infrared excess, one of the largest in our sample (Fig. 5). It was previously identified by Clarke et al. (2005) as an IR excess object based on matching *MSX* and Tycho-2 detections. Combining

2MASS and GLIMPSE IR photometry, with colors of $H - K = 0.23$ and $K - [8] = 1.40$, it appears consistent with a Be star (see Fig. 4 of Clarke et al. 2005). While a Be star might be expected to be an X-ray source, it is not consistent with the X-ray position, and is not noted as being a double, so this is probably a chance alignment.

6.51. CXB302

TYC 6849-01627-1 appears to be the optical counterpart to CXB302. There is very little information about this star. The optical colors would be consistent with a range of spectral types earlier than early G, depending on reddening, and the *JHK* colors suggest early F. It appears to show marginal irregular variability in ASAS.

6.52. CXB306

CXB306 coincides with HD 163613. This appears to be a normal early B supergiant. Its optical/IR colors are consistent with a single normal star, it shows no variability and there is no evidence for binarity. It was originally classified as B5 (Cannon & Pickering 1918–1924), and updated to B1 I–II by Hoffleit (1956). Its F_X/F_{bol} ratio is quite reasonable. The expected distance ranges from 2.8 kpc (B1 II) to 7.0 kpc (B1 Ia). Given that the GBS is observing out of the plane, and this source is at $b = -1.96^\circ$, less luminous stars seem most likely, since they imply shorter distances from the plane. For a distance of 2.8 kpc, the distance below the plane is about 80 pc, whereas for 7.0 kpc it is 240 pc. We then suggest this is a B1 II star at about 2.8 kpc in the Scutum-Centaurus arm.

6.53. CXB422

CXB422 is well matched with HD 315956. This is classified as an F2 star (Nesterov et al. 1995). Its parallax distance and brightness suggest a dwarf to giant luminosity class, and hence spectral class F2 III–V.

7. DISCUSSION

7.1. OB and Be stars

Four apparently normal OB stars, and two Be stars were found in our sample, all with very close matches between X-ray and optical positions. In addition, a third X-ray source (CXB296) was found near a Be star, but too far away to be a credible X-ray counterpart to it. There is every reason to believe the other six early type stars are all true optical counterparts to the X-ray sources.

Two of the OB stars CX31 and CXB8 have late-O spectral classes. They have quite high F_X/F_{bol} ratios, but still plausible for single, normal OB stars. Both have optical/IR colors consistent with normal stars, although CXB8 does have a mid-IR excess and appears to be a young object. CX31 has a rather hard X-ray spectrum (by the standards of our sample), but this is at least in part due to a higher N_H than the other OB stars in the sample, judging by its $(B - V)$ color. It remains possible that it is a more unusual object such as a colliding wind binary or low-luminosity X-ray binary. CX863 and CXB306 are slightly later in spectral class, early-B. Their F_X/F_{bol} ratios are lower, and quite typical of OB stars. CXB306 has normal stellar colors. CX863 may have slightly redder colors than a single star, but this only marginally significant

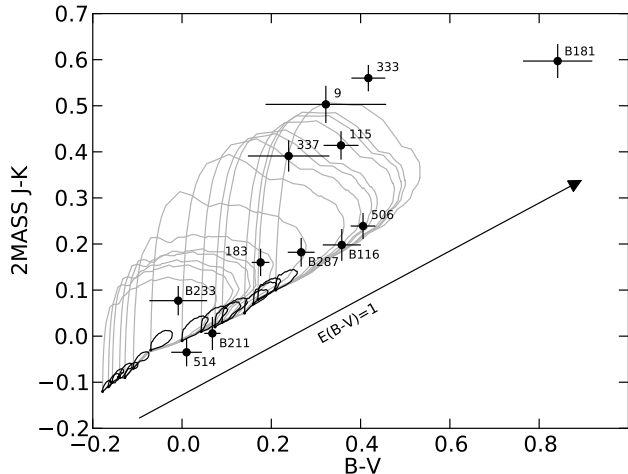


Figure 12. Optical/IR color-color diagram for spectroscopically classified late B and A stars in the sample. Black loops trace the effect of adding later-type main-sequence companions on the colors, for B3–A7 primaries. Grey loops correspond to companions 4 magnitudes brighter than a main-sequence star. In both cases, the loop is traced counter-clockwise from early-type companions to later types. This is adapted from Figure 5; see that figure for further explanation.

One of the GBS predictions was that ~ 9 Be X-ray binaries would be identified (Jonker et al. 2011). None have been found in the (nearby) Tycho-2 sample, but the sources predicted were expected to be further away and subject to more reddening, and so would not be expected to have Tycho-2 counterparts. Instead, the two Be stars we have found are fainter in X-rays. One, CX6, is an intermediate luminosity γ Cas system, possibly harboring a white dwarf. The other, CX33, is most likely a normal, single Be star.

7.2. Algol Candidates and other A stars

There are a surprising number of A stars in our sample. To some extent, this is a selection effect since our Tycho-2 sample is effectively an optical flux-limited sample and so has a larger sample volume for earlier spectral types. In most cases, as expected, there is evidence from IR colors and/or variability for a companion star, usually inferred to be larger in radius than the A star. Figure 12 shows just the spectroscopically confirmed late B and A stars from Figure 5. We show the B3–A7 main-sequence, together with two sets of loops, one corresponding to main-sequence companions of a range of spectral types, the other to more luminous companions. We see that the sources appear to divide into three groups. Neither of the two B9 stars, CX514 and CXB211 show evidence for an IR excess, although a main-sequence companion cannot be ruled out. CX183, CX506, CXB116, CXB233, and CXB287 all show weak excesses, suggesting main-sequence or mildly evolved companions. Finally CX9, CX115, CX333, CX337, and CXB181 all require luminous companions $\gtrsim 4$ mags above the main sequence.

The preponderance of evolved companions is not expected, since later type companions should not have had time to evolve off of the main-sequence. It could arise in two ways. First, where a large difference in spectral types is seen, it is possible that the later-type star is still a very active pre-main-sequence star, and so is larger than

it will eventually be. Secondly, an A star plus a late-type sub-giant or giant could be a typical Algol system.

CX115 is, indeed, a known eclipsing Algol. CX9 is also eclipsing and we propose that it is a new Algol candidate, and possibly a mass-transferring system. CX333 appears to show ellipsoidal variations suggesting a close, late-type companion in a 30 day period. It may be a long-period Algol. For the remainder of the sources, although a late-type companion is implied, there is no evidence that it is close.

7.3. Active late type stars

We attempt to distinguish active late-type stars (i.e. FGKM stars with very strong coronal emission) from those showing more normal coronal emission. Criteria for ‘activity’ include a high X-ray to optical flux ratio, hard X-ray spectra, or irregular variability.

The presence of radio emission would be a very powerful diagnostic as magnetically active stars usually follow the Güdel-Benz relation, whereas inactive stars are much weaker in the radio, while retaining significant X-ray emission (Forbrich et al. 2011, and references therein). Maccarone et al. (2012) looked for radio counterparts to GBS X-ray sources using the NVSS catalog (Condon et al. 1998). 12 matches were found with the original CX sources of Jonker et al. (2011), but none correspond to objects in this paper. Neither are any of the CXB sources in this paper detected by the NVSS. Unfortunately, while the NVSS is the deepest radio survey covering the whole GBS area, it is not sensitive enough to detect radio emission from these objects, as the Güdel-Benz relation would predict that all of the sources considered in this paper would fall well below the 2.5 mJy sensitivity of the NVSS.

Among the late-type stars, CX7 stands out. This is at or near coronal saturation and appears to be a very young K dwarf. CX352 is also distinguished by being the only W UMa contact binary in the sample. A few other stars show signs of strong activity. CX4 is a very active giant. CX10 and 12, and CXB5 are all active G or K stars with no luminosity class, showing high F_X/F_{bol} , quite hard X-ray spectra, and irregular variability. CX12, at least, appears to have a later type companion as well.

Finally we note two somewhat unusual F stars, both with moderately high F_X/F_{bol} . CX72 exhibited an unclassified outburst, with no other peculiarities. CX296 is unusual in its lack of peculiarities since F0 stars typically have quite weak X-ray emission; indeed, in Figure 4 it appears somewhat isolated, and lies an order of magnitude above other stars of the same spectral type.

7.4. Normal late type stars

Many of the late-type stars show no signs of strong activity; modest F_X/F_{bol} , and no variability. These include two giants, CX256 and CX632, and several dwarfs, CX26, CX205, CX275, and CX785. The remainder, CX91, CX402, CX485, CX916, and CXB422, have no luminosity classifications.

Our sample only included one Tycho-2 M dwarf, CXB93, together with its binary companion CXB36 which is not in the Tycho-2 catalog. Since the sample is selected by optical brightness, this is not surprising. The X-ray luminosities of these two stars are unremarkable, and if anything unusually low.

7.5. Chance alignments

After checking for known doubles, a few apparently single Tycho-2 stars are significantly offset from the nearby *Chandra* source, and these remain as probable chance alignments. These are CX59, CX156, CX360, CX388, CX622, CXB17, and CXB296. CXB296 is a particularly interesting case since it appears to lie near a Be star, yet that star rather securely is not the detected X-ray source. In addition, CX77 seems likely to not be associated with either HD 157571 or the star close to it, bringing us to a total of eight likely coincidences. There are additionally a few objects for which a real match could not be ruled out at the 95% confidence level, but which may nonetheless be close coincidences.

We estimated in Section 2.3 that there should be about 5 true coincidences in our sample. While finding 8 is not a substantial excess, with the high incidence of binarity among field stars, it is likely that some of these could be undetected resolved binary companions.

8. CONCLUSIONS

We have examined the properties of 69 stars from the Galactic Bulge Survey (Jonker et al. 2011, Jonker et al. in preparation) which match with Tycho-2 stars. All have quite low F_X/F_{opt} ratios in the range $10^{-6} - 10^{-2}$, and can be adequately explained without invoking compact companions. The sample includes one case where we appear to detect a resolved companion rather than the Tycho-2 star, and a further eight which appear to be chance alignments. This is comparable to the expectation of five coincidences and may include a few more undetected resolved companions.

The hot stars include two Be stars, one of which is a γ Cas analog. The remaining four spectroscopically identified OB stars show $F_X/F_{\text{bol}} \sim 10^{-7}$ as is commonly found for X-rays from the winds of these stars.

A substantial fraction of our sources, 12 objects out of 38 that have spectroscopic classifications, are A stars. One of these is a known Algol, V846 Oph, and the others include a disproportionate number of objects showing infrared excesses, and we expect that the X-rays in most or all of these objects come from cooler companions. These systems appear divided between some with very pronounced IR excesses that appear to have sub-giant or giant companions, and others with weaker or no IR excess consistent with main-sequence or mildly evolved companions.

Among the late-type stars a few stand out as having high F_X/F_{bol} ratios, and hard X-ray spectra implying high temperature coronae. These include the active giant, CX4, and a young K dwarf, CX7. Several other stars show quite high levels of activity.

The remainder of the late-type stars have lower F_X/F_{bol} ratios, and typically no evidence for variability. Some of these sources are rather close, in particular the one M dwarf in our sample, CXB93, and the modest X-ray luminosities implied can be accounted for by normal coronal emission.

This work was supported by the National Science Foundation under Grant No. AST-0908789 and by grant GO2-13044B from the Smithsonian Astrophysical Observatory. P.G.J. and G.N. acknowledge support from the

Netherlands Organisation for Scientific Research. D.S. acknowledges an STFC Advanced Fellowship. T.J.M. thanks STFC for support via a rolling grant to the University of Southampton. R.I.H. would like to thank the Universities of Warwick and Southampton, and SRON, the Netherlands Institute for Space Research in Utrecht for their hospitality while much of this work was being done.

This publication makes use of data products from the Two Micron All Sky Survey, which is a joint project of the University of Massachusetts and the Infrared Processing and Analysis Center/California Institute of Technology, funded by the National Aeronautics and Space Administration and the National Science Foundation. This research has made use of the SIMBAD database, operated at CDS, Strasbourg, France, and NASA's Astrophysics Data System. Finally we are very grateful to Dr. Eric Mamajek for making available his compilation of stellar colors and temperatures for dwarf stars.

Facilities: ASAS, CTIO:2MASS, CXO (ACIS), HIP-PARCOS.

REFERENCES

- Antokhin, I. I., Rauw, G., Vreux, J.-M., van der Hucht, K. A., & Brown, J. C. 2008, *A&A*, 477, 593
- Barbier-Brossat, M., & Figon, P. 2000, *A&AS*, 142, 217
- Berghöfer, T. W., Schmitt, J. H. M. M., Danner, R., & Cassinelli, J. P. 1997, *A&A*, 322, 167
- Bidelman, W. P. 1985, *ApJS*, 59, 197
- Brancewicz, H. K., & Dworak, T. Z. 1980, *Acta Astron.*, 30, 501
- Cannon, A. J., & Mayall, M. W. 1949, *Annals of Harvard College Observatory*, 112, 1
- Cardelli, J. A., Clayton, G. C., & Mathis, J. S. 1989, *ApJ*, 345, 245
- Coe, M. J. 2000, *IAU Colloq. 175: The Be Phenomenon in Early-Type Stars*, 214, 656
- Cohen, D. H., Cassinelli, J. P., & Macfarlane, J. J. 1997, *ApJ*, 487, 867
- Cox, A. N. (Ed.) 2000, *Allen's Astrophysical Quantities*, 4th Edn., AIP Press
- Bohlin, R. C., Savage, B. D., & Drake, J. F. 1978, *ApJ*, 224, 132
- Budding, E., Erdem, A., Çiçek, C., et al. 2004, *A&A*, 417, 263
- Cannon, A. J., Pickering, E. M. 1918–1924, *Ann. Astron. Obs. Harv. Coll.*, 91–99
- Cannon, A. J. 1925–1936, *Ann. Astron. Obs. Harv. Coll.*, 100, 1–6
- Churchwell, E., Babler, B. L., Meade, M. R., et al. 2009, *PASP*, 121, 213
- Clarke, A. J., Oudmaijer, R. D., & Lumsden, S. L. 2005, *MNRAS*, 363, 1111
- Condon, J. J., Cotton, W. D., Greisen, E. W., et al. 1998, *AJ*, 115, 1693
- Crampton, D. 1971, *AJ*, 76, 260
- Fabricsius, C., Høg, E., Makarov, V. V., et al. 2002, *A&A*, 384, 180
- Fabricsius, C., Makarov, V. V., Knude, J., & Wycoff, G. L. 2002, *A&A*, 386, 709
- Farrell, S. A., Gosling, A. J., Webb, N. A., et al. 2010, *A&A*, 523, A50
- Feigelson, E. D., Getman, K., Townsley, L., et al. 2005, *ApJS*, 160, 379
- Fitzgerald, M. P. 1970, *A&A*, 4, 234
- Forbrich, J., Wolk, S. J., Güdel, M., et al. 2011, *16th Cambridge Workshop on Cool Stars, Stellar Systems, and the Sun*, 448, 455
- Garrison, R. F., Hiltner, W. A., & Schild, R. E. 1977, *ApJS*, 35, 111
- Gillessen, S., Eisenhauer, F., Trippe, S., et al. 2009, *ApJ*, 692, 1075
- Gondoin, P. 2005, *A&A*, 444, 531
- Gonzalez, O. A., Rejkuba, M., Zoccali, M., Valenti, E., & Minniti, D. 2011, *A&A*, 534, A3
- Gonzalez, O. A., Rejkuba, M., Zoccali, M., et al. 2012, *A&A*, 543, A13

- Gray, A. D. 1994, *MNRAS*, 270, 847
- Güdel, M. 2004, *A&A Rev.*, 12, 71
- Güdel, M., & Nazé, Y. 2009, *A&A Rev.*, 17, 309
- Hiltner, W. A. 1956, *ApJS*, 2, 389
- Høg, E., Fabricius, C., Makarov, V. V., et al. 2000a, *A&A*, 355, L27
- Høg, E., Fabricius, C., Makarov, V. V., et al. 2000b, “Guide to the Tycho-2 Catalog”, Copenhagen University Observatory
- Hoffleit, D. 1956, *ApJ*, 124, 61
- Hong, J., van den Berg, M., Schlegel, E. M., et al. 2005, *ApJ*, 635, 907
- Houk, N. 1982, Michigan Catalogue of Two-dimensional Spectral Types for the HD stars. Volume 3. Declinations -40° to -26° , by Houk, N.. Ann Arbor, MI(USA): Department of Astronomy, University of Michigan, 12 + 390 p.,
- Hu, J. Y., Slijkhuys, S., de Jong, T., & Jiang, B. W. 1993, *A&AS*, 100, 413
- Hünsch, M., Schmitt, J. H. M. M., & Voges, W. 1998, *A&AS*, 127, 251
- Jonker, P. G., Bassa, C. G., Nelemans, G., et al. 2011, *ApJS*, 194, 18
- Koen, C., Kilkeny, D., van Wyk, F., & Marang, F. 2010, *MNRAS*, 403, 1949
- van Leeuwen, F. 2007, *A&A*, 474, 653
- Levenhagen, R. S., & Leister, N. V. 2006, *MNRAS*, 371, 252
- Lopes de Oliveira, R., Motch, C., Haberl, F., Negueruela, I., & Janot-Pacheco, E. 2006, *A&A*, 454, 265
- Maccarone, T. J., Torres, M. A. P., Britt, C. T., et al. 2012, *MNRAS*, 426, 3057
- MacConnell, D. J., & Bidelman, W. P. 1976, *AJ*, 81, 225
- Maggio, A., Sciortino, S., Vaiana, G. S., et al. 1987, *ApJ*, 315, 687
- Majaess, D. J., Turner, D. G., & Lane, D. J. 2009, *MNRAS*, 398, 263
- Malkov, O. Y., Oblak, E., Snegireva, E. A., & Torra, J. 2006, *A&A*, 446, 785
- Mason, B. D., Wycoff, G. L., Hartkopf, W. I., Douglass, G. G., & Worley, C. E. 2001, *AJ*, 122, 3466
- Merrill, P. W., Humason, M. L., & Burwell, C. G. 1925, *ApJ*, 61, 389
- Motch, C., Haberl, F., Dennerl, K., Pakull, M., & Janot-Pacheco, E. 1997, *A&A*, 323, 853
- Motch, C., Lopes de Oliveira, R., Negueruela, I., Haberl, F., & Janot-Pacheco, E. 2007, *Active OB-Stars: Laboratories for Stellare and Circumstellar Physics*, 361, 117
- Neese, C. L., & Yoss, K. M. 1988, *AJ*, 95, 463
- Nesterov, V. V., Kuzmin, A. V., Ashimbaeva, N. T., et al. 1995, *A&AS*, 110, 367
- Nordstrom, B., Stefanik, R. P., Latham, D. W., & Andersen, J. 1997, *A&AS*, 126, 21
- Otero, S. A., Hoogeveen, G. J., & Wils, P. 2006, *Information Bulletin on Variable Stars*, 5674
- Owocik, S. P., & Cohen, D. H. 2001, *ApJ*, 559, 1108
- Pallavicini, R., Golub, L., Rosner, R., et al. 1981, *ApJ*, 248, 279
- Parthasarathy, M., Vijapurkar, J., & Drilling, J. S. 2000, *A&AS*, 145, 269
- Piquard, S., Halbwachs, J.-L., Fabricius, C., et al. 2001, *A&A*, 373, 576
- Pojmanski, G. 2002, *Acta Astron.*, 52, 397
- Pollock, A. M. T. 2007, *A&A*, 463, 1111
- Porter, J. M., & Rivinius, T. 2003, *PASP*, 115, 1153
- Pease, D. O., Drake, J. J., & Kashyap, V. L. 2006, *ApJ*, 636, 426
- Raharto, M., Hamajima, K., Ichikawa, T., Ishida, K., & Hidayat, B. 1984, *Annals of the Tokyo Astronomical Observatory*, 19, 469
- Rauscher, E., & Marcy, G. W. 2006, *PASP*, 118, 617
- Richichi, A., Fors, O., & Mason, E. 2008, *A&A*, 489, 1441
- Saito, R. K., Hempel, M., Minniti, D., et al. 2012, *A&A*, 537, A107
- Samus, N. N., Durlevich, O. V., & et al. 2009, *VizieR Online Data Catalog*, 1, 2025
- Sana, H., Rauw, G., Nazé, Y., Gosset, E., & Vreux, J.-M. 2006, *MNRAS*, 372, 661
- Savage, B. D., Massa, D., Meade, M., & Wesselius, P. R. 1985, *ApJS*, 59, 397
- Schmitt, J. H. M. M., Fleming, T. A., & Giampapa, M. S. 1995, *ApJ*, 450, 392
- Sidoli, L., Belloni, T., & Mereghetti, S. 2001, *A&A*, 368, 835
- Siebert, A., Williams, M. E. K., Siviero, A., et al. 2011, *AJ*, 141, 187
- Singh, K. P., Drake, S. A., & White, N. E. 1996, *AJ*, 111, 2415
- Skiff, B. A. 2011, *General Catalogue of Stellar Spectral Classifications*, *VizieR Online Catalog*
- Skrutskie, M. F., Cutri, R. M., Stiening, R., et al. 2006, *AJ*, 131, 1163
- Skumanich, A. 1972, *ApJ*, 171, 565
- Steele, I. A., Negueruela, I., & Clark, J. S. 1999, *A&AS*, 137, 147
- Stephenson, C. B., & Sanduleak, N. 1975, *AJ*, 80, 972
- Stevens, I. R., Blondin, J. M., & Pollock, A. M. T. 1992, *ApJ*, 386, 265
- Straižys, V., & Lazauskaitė, R. 2009, *Baltic Astronomy*, 18, 19
- Straižys, V., & Kuriliene, G. 1981, *Ap&SS*, 80, 353
- Suárez, O., García-Lario, P., Manchado, A., et al. 2006, *A&A*, 458, 173
- Suchkov, A. A., Makarov, V. V., & Voges, W. 2003, *ApJ*, 595, 1206
- Svechnikov, M. A., & Kuznetsova, E. F. 2004, *VizieR Online Data Catalog*, 5124, 0
- Torres, C. A. O., Quast, G. R., da Silva, L., et al. 2006, *A&A*, 460, 695
- Vaiana, G. S., Cassinelli, J. P., Fabbiano, G., et al. 1981, *ApJ*, 245, 163
- Vijapurkar, J., & Drilling, J. S. 1993, *ApJS*, 89, 293
- Walborn, N. R. 1973, *AJ*, 78, 1067
- Wright, N. J., Drake, J. J., & Civano, F. 2010, *ApJ*, 725, 480
- Wright, N. J., Drake, J. J., Mamajek, E. E., & Henry, G. W. 2011, *ApJ*, 743, 48
- Zacharias, N., Finch, C., Girard, T., et al. 2010, *AJ*, 139, 2184